



The Paleocene of Antarctica: Dinoflagellate cyst biostratigraphy, chronostratigraphy and implications for the palaeo-Pacific margin of Gondwana



V. Bowman^{a,*}, J. Ineson^b, J. Riding^c, J. Crame^a, J. Francis^a, D. Condon^c, R. Whittle^a, F. Ferraccioli^a

^a British Antarctic Survey, High Cross, Madingley Road, Cambridge CB3 0ET, UK

^b Geological Survey of Denmark and Greenland, Øster Volgade 10, DK, 1350 Copenhagen K, Denmark

^c British Geological Survey, Environmental Science Centre, Keyworth, Nottingham NG12 5GG, UK

ARTICLE INFO

Article history:

Received 15 June 2015

Received in revised form 16 October 2015

Accepted 26 October 2015

Available online 23 December 2015

Handling Editor: A.S. Collins

Keywords:

Cretaceous–Paleocene

Antarctic Peninsula

Gondwana

Biostratigraphy

Palaeogeography

ABSTRACT

The Paleocene (66–56 Ma) was a critical time interval for understanding recovery from mass extinction in high palaeolatitudes when global climate was warmer than today. A unique sedimentary succession from Seymour Island (Antarctic Peninsula) provides key reference material from this important phase of the early Cenozoic. Dinoflagellate cyst data from a 376 m thick stratigraphical section, including the Cretaceous–Paleogene boundary, is correlated with biozones from New Zealand, the East Tasman Plateau and southeastern Australia. A detailed age model is suggested for the López de Bertodano (LDBF) and Sobral (SF) formations based on dinoflagellate cyst biostratigraphy and U–Pb dating of zircons, supported by correlated magnetostratigraphy and strontium isotope values from macrofossils. The top of the LDBF is confirmed as latest Maastrichtian to earliest Danian (~66.2–65.65 Ma) in age. The overlying SF is mostly Danian in age, with an inferred hiatus near the top overlain by sediments dated as ?late Thanetian. Rare *Apectodinium homomorphum* first appear in the uppermost SF; the earliest *in situ* record from Antarctica. The distribution of marine and terrestrial fossils from uppermost Cretaceous to Eocene sediments in Patagonia, Antarctica, New Zealand and Australia required both sea and land connections between these fragments of Gondwana. Fossil evidence and reconstructions of Antarctic palaeogeography and palaeotopography reveal evidence for persistent embayments in the proto-Weddell and Ross Sea regions at this time. We conclude that a coastal dispersal route along the palaeo-Pacific margin of Gondwana could explain the fossil distribution without requiring a transAntarctic strait or closely spaced archipelago. A region in the West to East Antarctic boundary zone, elevated until the early Paleogene, perhaps acted as a site for high elevation ice caps. This supports fossil, geochemical and sedimentological evidence for cold climate intervals and significant sea level falls during the Maastrichtian and Paleocene.

© 2015 The Authors. Published by Elsevier B.V. on behalf of International Association for Gondwana Research.

This is an open access article under the CC BY license (<http://creativecommons.org/licenses/by/4.0/>).

1. Introduction

The Paleocene (66–56 Ma) was a time of cooler global climate between the greenhouse phases of the mid Cretaceous and Eocene (Zachos et al., 2001; Royer, 2006; Zachos et al., 2008). During the Paleocene, global biotas changed significantly in response to several major environmental perturbations. It is possible that a period of intense volcanic outgassing during the latest Maastrichtian to earliest Danian from the Indian Deccan Peninsula had global effects (Chenet et al., 2009; Courtillot and Fluteau, 2010; Schoene et al., 2014). Furthermore, there was a major meteorite impact at the Cretaceous–Paleogene (K–Pg) boundary coincident with mass extinctions of marine plankton and major changes in terrestrial vegetation (Schulte et al., 2010; Molina, 2015). There is a growing volume of evidence to suggest that some key components of the modern Southern Ocean

marine fauna had their origins in the Early Cenozoic (Crame et al., 2014). However, despite recent work on Paleocene successions in the low and mid palaeolatitudes (e.g. Hollis et al., 2012, 2014; Storme et al., 2014), little is known about the implications of these events for high southern latitude biota, or indeed what they can tell us about Antarctic palaeogeography in the final phases of Gondwana fragmentation.

The only onshore exposure of strata of this age in the Antarctic is on ice-free Seymour Island, at ~64° South, in the James Ross Basin at the tip of the Antarctic Peninsula (Fig. 1; Elliot et al., 1994; Montes et al., 2010; Bowman et al., 2012, 2013a). During the Cretaceous and Paleogene, sediments of the Marambio Group that now form much of the island were being deposited in mid shelf and deltaic settings in a back-arc basin at a similar palaeolatitude (Lawver et al., 1992; Hathway, 2000; Crame et al., 2004; Martos et al., 2014). The succession is highly fossiliferous, is suitable for magnetostratigraphical analysis (Tobin et al., 2012), and has several ash beds (airfall tuffs) preserved above the K–Pg boundary (Fig. 2).

* Corresponding author. Tel.: +44 1223 221400; fax: +44 1223 362616.
E-mail address: vanessa.bowman@bas.ac.uk (V. Bowman).

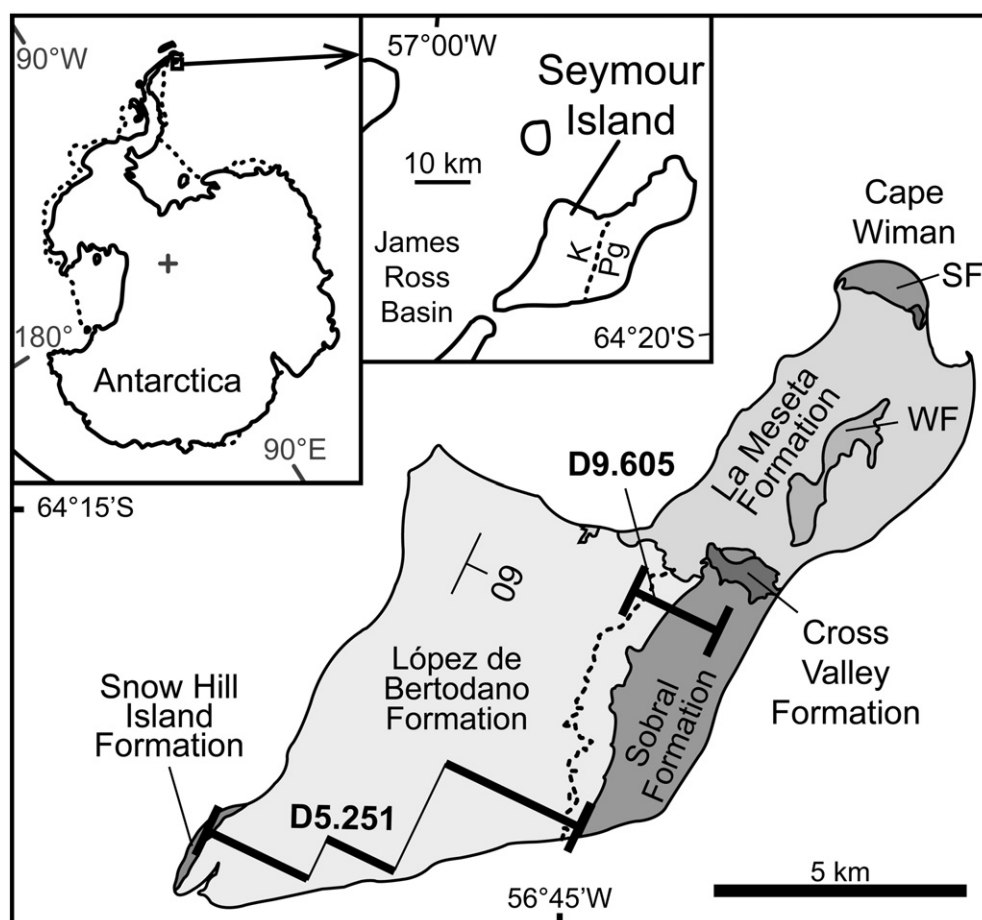


Fig. 1. Locality and geological map of Seymour Island, James Ross Basin, northeastern tip of the Antarctic Peninsula. Geology after Montes et al. (2010). K, Cretaceous; Pg, Paleogene; SF, Sobral Formation; WF, Weddell Formation. Approximate position of British Antarctic Survey stratigraphical section lines D9.605 (composite of section lines D9.600, D9.601, D9.602, D9.603 and D9.604) and D5.251 (composite of D5.201, D5.212, D5.215, D5.218, D5.219, D5.220, D5.222 and D5.229; after Bowman et al., 2012, 2013a, 2014).

Previous work has refined the age of the oldest part of the Seymour Island succession (the uppermost Snow Hill Island Formation and the López de Bertodano Formation) as Maastrichtian to earliest Danian using dinoflagellate cyst biostratigraphy correlated to magnetostratigraphy and strontium isotope stratigraphy (Askin, 1988a; McArthur et al., 1998; Bowman et al., 2012; Tobin et al., 2012; Bowman et al., 2013a). A new measured section through the uppermost López de Bertodano Formation, across the K–Pg boundary, and through the overlying Sobral Formation in the central part of the island (Fig. 1) is the focus of this paper.

We provide a detailed age model for the succession, across the K–Pg boundary into the Paleocene in order to provide a robust stratigraphical context for this key reference section. The emphasis is on dinoflagellate cyst biostratigraphy and correlating significant bioevents with known biozonation schemes in the mid to high southern latitudes that have been correlated to the International Timescale (Gradstein et al., 2012) (Partridge, 2006; Bijl et al., 2013; Crouch et al., 2014). The overall age model includes previous work on palynomorphs and other fossil groups (Askin, 1988a,b; Harwood, 1988; Huber, 1988; Wrenn and Hart, 1988; Zinsmeister and Macellari, 1988; Olivero and Zinsmeister, 1989; Olivero and Medina, 2000; Thorn et al., 2009; Crame et al., 2014; Witts et al., 2015). Supporting evidence also includes magnetostratigraphical tie-points (Tobin et al., 2012; Vandenberghe et al., 2012), U–Pb isotope dates from zircons extracted from airfall tuff horizons (this study) and strontium isotope analyses from macrofossils (McArthur et al., 1998). Close taxonomic similarity of the Paleocene dinoflagellate cyst floras across remnants of the palaeo-Pacific margin of Gondwana provides

a broader context for this study. This involves analysis of the final fragmentation of Gondwana and the Late Cretaceous to Eocene palaeogeographical and palaeotopographical evolution of Antarctica.

2. Field and palynological methods

A new 376 m composite section was measured and sampled throughout the uppermost López de Bertodano and Sobral formations in central Seymour Island (D9.605; Figs. 1, 2). This is located at 64°16′17.28″S, 056°43′1.38″W to 64°16′16.02″S, 056°40′53.16″W. The section was measured using a Jacob's staff and Abney level with finer intervals established by tape measure. All sub-sections were correlated lithologically in the field. The uppermost López de Bertodano and Sobral formations strike ~020° north-northeast, and gently dip (~9°) towards the east-southeast (Fig. 1). The López de Bertodano Formation crops out in the southern and central parts of the island. It is overlain unconformably by the Sobral Formation, the upper part of which is also exposed on the northern tip of the island at Cape Wiman (Fig. 1). Section D9.605 comprises several sub-sections (D9.600 to D9.604) that, when combined, form a contiguous succession through the part of the island where the Sobral Formation is most fully developed (Fig. 2). Between each sub-section, individual beds were traced along strike in order to avoid areas of poor exposure in the field (e.g. across mud-filled valleys) to ensure accuracy of measurement and sampling along a continuous stratigraphical section.

The base of section D9.605 overlaps with the top of section D5.251 (Thorn et al., 2009; Bowman et al., 2012, 2013a,b; Witts et al., 2015),

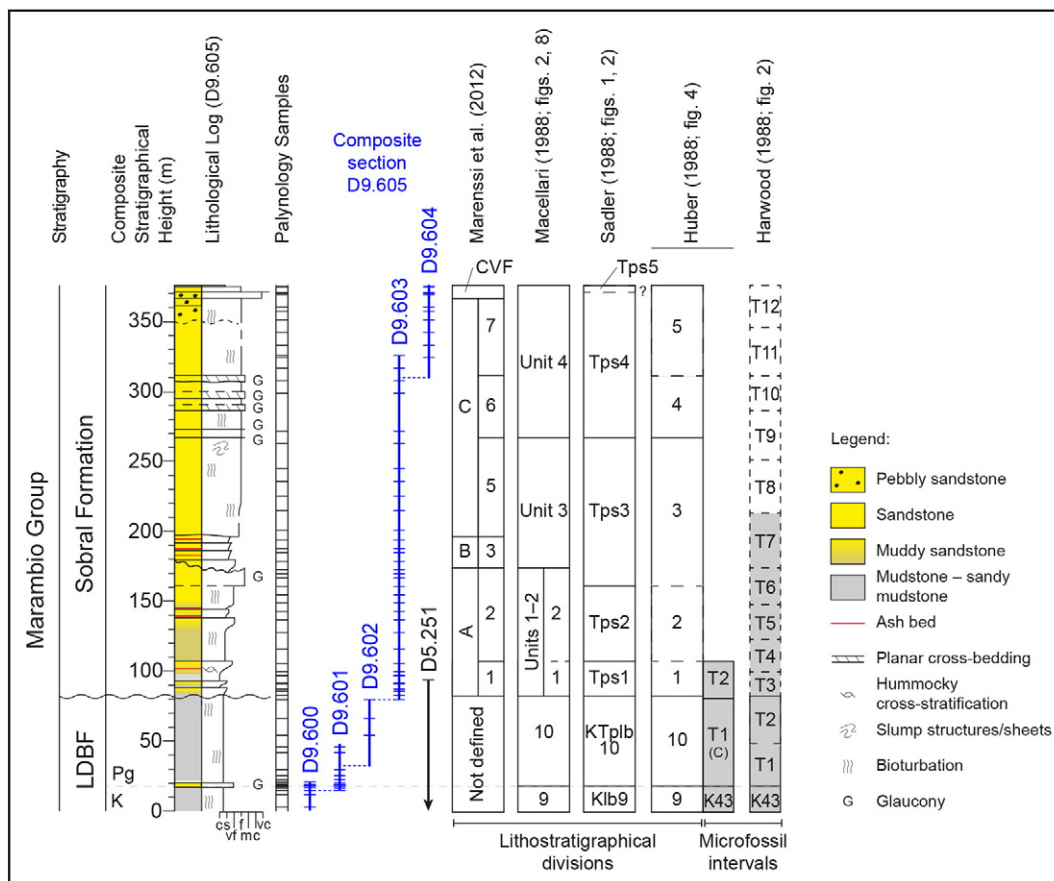


Fig. 2. Stratigraphy and summary lithological log for section D9.605 showing palynology sample horizons, sub-sections and correlation to previous measured section D5.251, lithostratigraphical divisions and microfossil sampling intervals (see Supplementary Table 1). The succession continues below and above D9.605. Numbered microfossil intervals as defined by Huber (1988) and Harwood (1988) are correlated to D9.605 to utilise this previous work on silicoflagellate and foraminifera biostratigraphy. Grey shaded intervals are those where microfossils were extracted by these authors. Dashed lines between units and microfossil intervals represent less certain placement of boundaries against D9.605. c, clay; s, silt; vf, very fine sand; f, fine sand; m, medium sand; cs, coarse sand; vc, very coarse sand. Dashed wavy line represents the inferred hiatus discussed herein. LDBF, López de Bertodano Formation; CVF, Cross Valley Formation; K, Cretaceous; Pg, Paleogene; C, dissolution facies (Huber, 1988).

providing higher resolution data for the K–Pg transition and lowermost Danian part of the succession (Fig. 2). The two sections provide a continuous stratigraphical record across the south-central part of Seymour Island, and are correlated on the basis of lithology using the K–Pg boundary as a tie-point and assuming approximately planar bedding and continuous sedimentation.

Sixty-seven sediment samples were collected throughout section D9.605 and processed for palynomorphs using standard laboratory techniques by Palytech Processing Ltd., Birkenhead, UK (e.g. Wood et al., 1996). To refine the position of the K–Pg boundary in section D9.605, palynomorph samples were collected throughout the fine-grained sediments of the uppermost López de Bertodano Formation, with several concentrated within the glaucony-rich beds ~18 m above the base of the section.

Dry bulk sediment (10 g per sample) was sieved at 10 µm and treated with hydrochloric and hydrofluoric acids, followed by oxidation between 2 and 4 minutes in nitric acid. Final separation of inorganic and organic fractions was completed using zinc chloride centrifugation and swirling. Concentration of palynomorphs was achieved by top sieving at 180 µm, leaving organic material between 10 and 180 µm for mounting onto the slide. To achieve a reasonable palynomorph density, organic residue from between 0.5 and 2.0 g of sediment was mounted on each microscope slide depending on recovery. This residue was permanently mounted onto glass microscope slides with polyvinyl alcohol as the dispersant and adhesive. All slides are curated and stored at the British Antarctic Survey, Cambridge, UK.

Microscope slides were analysed on a Leica DM750P transmitted light microscope using phase contrast. In the D9.605 samples, the marine palynomorphs encountered were counted on regularly spaced transects across the entire width of the coverslip until a sum of at least 300 specimens was reached. Where recovery was insufficient, all mounted material was scanned, up to two slides per sample. For the slides where recovery was good and the count was achieved on a single slide, the remainder of that slide was scanned for additional rare taxa, after the count was completed. Rare dinoflagellate cysts were considered reworked if they were relatively more thermally mature, significantly torn or fragmented (except for *Trithyrodinium evittii*, which is commonly fragmented *in situ*), or isolated beyond their common range.

Two ash beds were sampled from section D9.605 at 136.8 m (sample D9.085.1) and 142.8 m (D9.087.1), processed for zircon and subsequently analysed for U–Pb geochronology. Ash beds were processed for heavy minerals using conventional methods (magnetics and gravity) to derive a zircon concentrate, after which a subset was selected for analyses by the isotope dilution (ID) thermal ionisation mass spectrometry (TIMS) method using the chemical abrasion (CA) pre-treatment method (Mattinson, 2005) for the effective elimination of Pb-loss. ID was performed using the EARTH TIME ET535 tracer, which has been gravimetrically calibrated (Condon et al., 2015; McLean et al., 2015) such that derived dates and uncertainties are to be considered absolute and comparable to dates presented in GTS 2012 (Gradstein et al., 2012). Details of correction for laboratory blank and intermediate daughter

disequilibrium follow those outlined in Singer et al. (2014). The uncertainties reflect the following sources: analytical/analytical + tracer solution + decay constants; the latter value is the total uncertainty in each case.

3. Geological setting and sedimentology

The López de Bertodano and Sobral formations are part of the Marambio Group in the James Ross Basin, and have a combined stratigraphical thickness on Seymour Island of ~1500 m (Crame et al., 2004; Bowman et al., 2012, 2013a). This thick sedimentary package formed as major rivers brought huge volumes of fine-grained sediment into the shallow marine basin from a vegetated volcanic arc to the west, now the Antarctic Peninsula (Pirrie et al., 1992; Bowman et al., 2014; Martos et al., 2014). The coastline extended northwards and there was a functioning land bridge with Patagonia until the Early Eocene (~50 Ma) (Crame et al., 2004; Olivero et al., 2008; Eagles and Jokat, 2014; Reguero et al., 2014). Two Ocean Drilling Program cores at Sites 689 and 690 to the east in the Weddell Sea at Maud Rise also include a sedimentary record of latest Cretaceous to Paleogene deposition in this region, but consist of palynologically-barren white calcareous ooze (Barker et al., 1988; Mohr, 1990; Thomas et al., 1990).

The uppermost López de Bertodano Formation has been divided into informal lithostratigraphical units by Sadler (1988), with K1b9 (Unit 9) reaching the K–Pg boundary and KTplb10 (Unit 10) comprising the remainder of the formation up to the unconformable contact with the overlying Sobral Formation (Fig. 2). The overlying Sobral Formation has been similarly divided into lithostratigraphical units, which vary in their definitions (Macellari, 1988; Sadler, 1988; Marenssi et al., 2012). Each of these lithostratigraphical schemes has been correlated to composite section D9.605 using sedimentology in order to accurately relate previous siliceous microfossil and foraminiferal biostratigraphy (Harwood, 1988; Huber, 1988) (Fig. 2, Supplementary Methodology).

Across and above the K–Pg boundary, the uppermost López de Bertodano Formation is similar to the rest of the underlying formation comprising relatively homogeneous and unconsolidated marine clayey-silts and silty-clays, with beds of calcareous concretions, often following thin burrowed sand deposits (Macellari, 1984; Bowman et al., 2012; Olivero, 2012). It has been interpreted broadly as a transgressive shelf succession, much of the formation representing mid-shelf conditions above a basal estuarine unit (Macellari, 1988; Olivero et al., 2007, 2008; Olivero, 2012).

The uppermost ~300 m of the formation are characterised by an increasing content of glaucony, typically concentrated in thin sandy, fossiliferous units that form resistant ridges; the K–Pg boundary unit is an example of one such unit. Although the glaucony of the latter unit has not been studied petrographically, a preliminary petrographic and geochemical study of an analogous interval about 190 m below the K–Pg concluded that the glaucony was autochthonous in nature. This suggests that although the López de Bertodano Formation represents an expanded Maastrichtian–earliest Paleocene section overall, deposition on the shelf was interrupted by periods of slow, condensed sedimentation.

The K–Pg boundary on Seymour Island occurs within the upper López de Bertodano Formation, where it is located near the base of a prominent composite glaucony-rich unit, within what has been termed the “Lower Glauconite” (Zinsmeister, 1998; Elliot et al., 1994). The boundary is positioned within the lower few metres of this unit on the basis of dinoflagellate cyst and macrofaunal biostratigraphy and an iridium anomaly (Askin, 1988b; Elliot et al., 1994; Zinsmeister, 1998; Bowman et al., 2012, 2013a; Witts et al., 2015). The outcrop of the K–Pg boundary glaucony unit extends ~ 5.5 km along strike (Fig. 1). The base of the unit is typically gradational (Elliot et al., 1994; Zinsmeister, 1998) though sharp, erosional contacts are observed in places. Since there is minimal change in the dinoflagellate cyst record across this contact (Bowman et al., 2012; this study), it is likely to

represent a laterally variable facies boundary rather than a significant hiatus. The uniformity of the bioturbated glauconitic muddy sands through this interval suggests that sedimentation was relatively continuous across the K–Pg boundary itself (see also Elliot et al., 1994). The abundance of glaucony within this unit as a whole has been suggested to indicate a period of slow, condensed sedimentation (e.g. Macellari, 1988) though detailed petrographic study of these sediments to determine the origin of the glaucony is presently lacking.

The Sobral Formation, the main focus of this paper, overlies an erosional unconformity that locally cuts into the López de Bertodano Formation for up to several tens of metres, indicative of a significant fall in relative sea level and fluvial erosion (Macellari, 1988; Sadler, 1988; Santillana and Marenssi, 1997; Marenssi et al., 2012; Olivero, 2012). There is an overall coarsening-upward, regressive trend through the Sobral Formation, reflecting eastward progradation of a marine delta (Macellari, 1988; Marenssi et al., 2012).

The lower ~115 m of the Sobral Formation (81–196 m in Fig. 2) consist of sediments that accumulated near the toe of the delta system, including prodeltaic mud-dominated facies showing evidence of slope instability (slump scars), and distal delta front facies characterised by bioturbated muddy very fine- to fine-grained sandstones with a rich molluscan fauna. A discrete interval (160–180 m on Fig. 2) is rich in glaucony of autochthonous origin, based on preliminary petrographic study (unpublished data), and records a period of slow sedimentation on the distal delta, probably the result of a significant rise in relative sea level (Macellari, 1988; Marenssi et al., 2012). The glaucony within the tidally cross-bedded sands higher up in the Sobral Formation (between ~265 and 312 m) is interpreted as being reworked (Macellari, 1988), and therefore this unit is not considered a site of glaucony formation. Much of the upper Sobral Formation (196–350 m on Fig. 2) represents more nearshore, higher energy deltaic facies, including bioturbated or cross-bedded well-sorted medium- to fine-grained sands/sandstones of the proximal delta front and delta platform.

A significant hiatus is inferred at ~350 m (Fig. 2) by the palynological data presented here. This precedes a marked change in facies where the uppermost ~25–30 m of the Sobral Formation (350–376 m in Fig. 2) is characterised by a heterogeneous succession of volcanoclastic matrix-rich conglomerates and burrowed or cross-bedded pebbly sandstones, interbedded locally with bioturbated heterolithic mudstones.

4. Dinoflagellate cyst biostratigraphy

Marine palynomorphs (dinoflagellate cysts, acritarchs and other marine algae) are well-preserved and abundant in 65 samples from section D9.605 (Fig. 3; Supplementary Table 1). Total dinoflagellate cysts counted per sample ranged between 155 and 760 (the mean was 349). Recovery was poor in only two sandy samples from the uppermost part of the section (D9.163.1 at 370.3 m and D9.167.1 at 375.3 m; Supplementary Table 1). A list of all fossil taxa recorded in the present study is included in Appendix A. Additional fossil taxa discussed herein are listed in Appendix B.

All *in situ* palynomorphs have undergone minimal thermal maturation and, without staining, required observation under phase contrast. The dinoflagellate cyst ranges are presented in Fig. 4. Observed lowest and highest occurrences (LOs and HOs respectively) do not necessarily represent inception or extinctions. Acritarchs and miscellaneous marine palynomorphs (e.g. *Palamblages* spp.) and terrestrially-derived palynomorphs (including freshwater algal and fungal spores) are also well-preserved.

The dinoflagellate cyst assemblages from section D9.605 include many taxa that are typical of the mid to high southern latitudes during this interval, for example, *Palaecocystodinium golzowense* and *Cerebrocysta waipawaensis* (see Crouch et al., 2014). Several taxa are cosmopolitan, including *Manumiella druggii*, *Trithyrodinium evittii* and *Palaoperidinium pyrophorum* (e.g. Heilmann-Clausen, 1985; Nøhr-Hansen and Dam, 1999; Mudge and Bujak, 2001; Bowman et al., 2012).

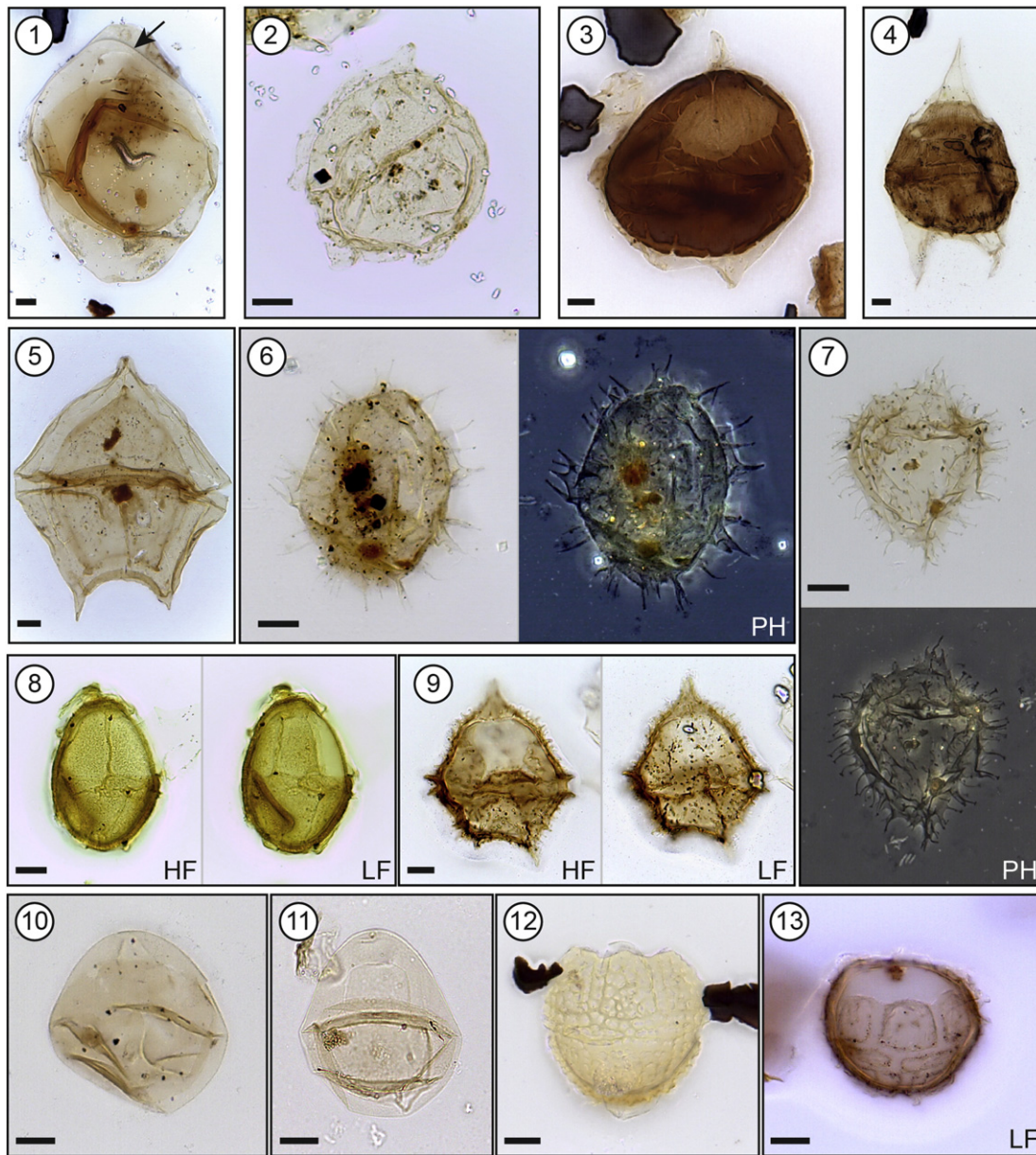


Fig. 3. Stratigraphically significant dinoflagellate cysts from the uppermost López de Bertodano Formation and overlying Sobral Formation, Seymour Island, Antarctica. British Antarctic Survey slide number, Leica DM750P stage and England Finder co-ordinates are given for each specimen. PH, phase contrast; LF, low focus; HF, high focus. Scale bar = 10 μ m. 1, *Manumiella druggii* with mesophragm (arrow), D9.007.1A, 262833, Y50-2; 2, *Senegalinium obscurum*, D9.030.1A, 080780, T69-2; 3, *Trithyrodinium evittii*, D9.051.1A, 138668, G63-4; 4, *Cerodinium striatum*, D9.129.1A, 084797, U69-0; 5, *Palaeoperidinium pyrophorum*, D9.129.1A, 123693, K65-1; 6, *Apectodinium* sp., D9.149.1A, 279745, P49-1; 7, *Apectodinium homomorphum*, D9.161.2A, 339776, S43-1; 8, *Impagidinium maculatum*, D9.151.1A, 243737, O52-0; 9, *Vozzhennikovia angulata*, presumed reworked, D9.150.1A, 082784, T69-0; 10, *Manumiella rotunda* end-member, reduced apical epicoel, D9.164.1A, 135753, Q64-1; 11, *Manumiella rotunda* end-member, expanded apical epicoel, D9.166.1A, 294828, X47-0; 12, *Eisenackia reticulata*, D9.166.1A, 240650, E53-3; 13, *Eisenackia margarita*, D9.166.1A, 192703, L58-1.

Here, we discuss the dinoflagellate cyst biostratigraphy from section D9.605 with reference to earlier work on Seymour Island (e.g. Askin, 1988a; Bowman et al., 2012). In addition, this is supported by studies from the mid to high southern palaeolatitudes, specifically, the eastern basins of New Zealand (Wilson, 1987, 1988; Crouch et al., 2014), south-eastern Australia (e.g. Helby et al., 1987; McMinn, 1988; Partridge, 2006) and the East Tasman Plateau (Bijl et al., 2013). Above the K–Pg boundary, the dinoflagellate cyst flora from D9.605 compares closely with that from the New Zealand Paleocene. Crouch et al. (2014) revised the biozonation scheme of Wilson (1984, 1987, 1988) based on several sections and cores from the east coast basins of New Zealand. Many of the key bioevents from New Zealand are recorded herein from Seymour Island.

4.1. Latest Maastrichtian and the K–Pg boundary

Dinoflagellate cyst range data and key bioevents from the interval of overlap between section D5.251 and section D9.605 described herein compare well, as expected (Bowman et al., 2012; Figs. 2, 4, 5). This allows the recognition of the latest Maastrichtian to earliest Danian *Manumiella druggii* Range Zone, the *Hystrichosphaeridium tubiferum* Acme Zone and the *Trithyrodinium evittii* Acme Zone in D9.605 (Fig. 6).

At the base of section D9.605, 11.85 m below the K–Pg boundary and within the upper part of Unit 9, a *Manumiella*-dominated assemblage is present (peaking at 68% of the dinoflagellate cysts). Consistent with previous work on the latest Maastrichtian of this succession, this lowermost part of the section represents the *Manumiella druggii* Range Zone

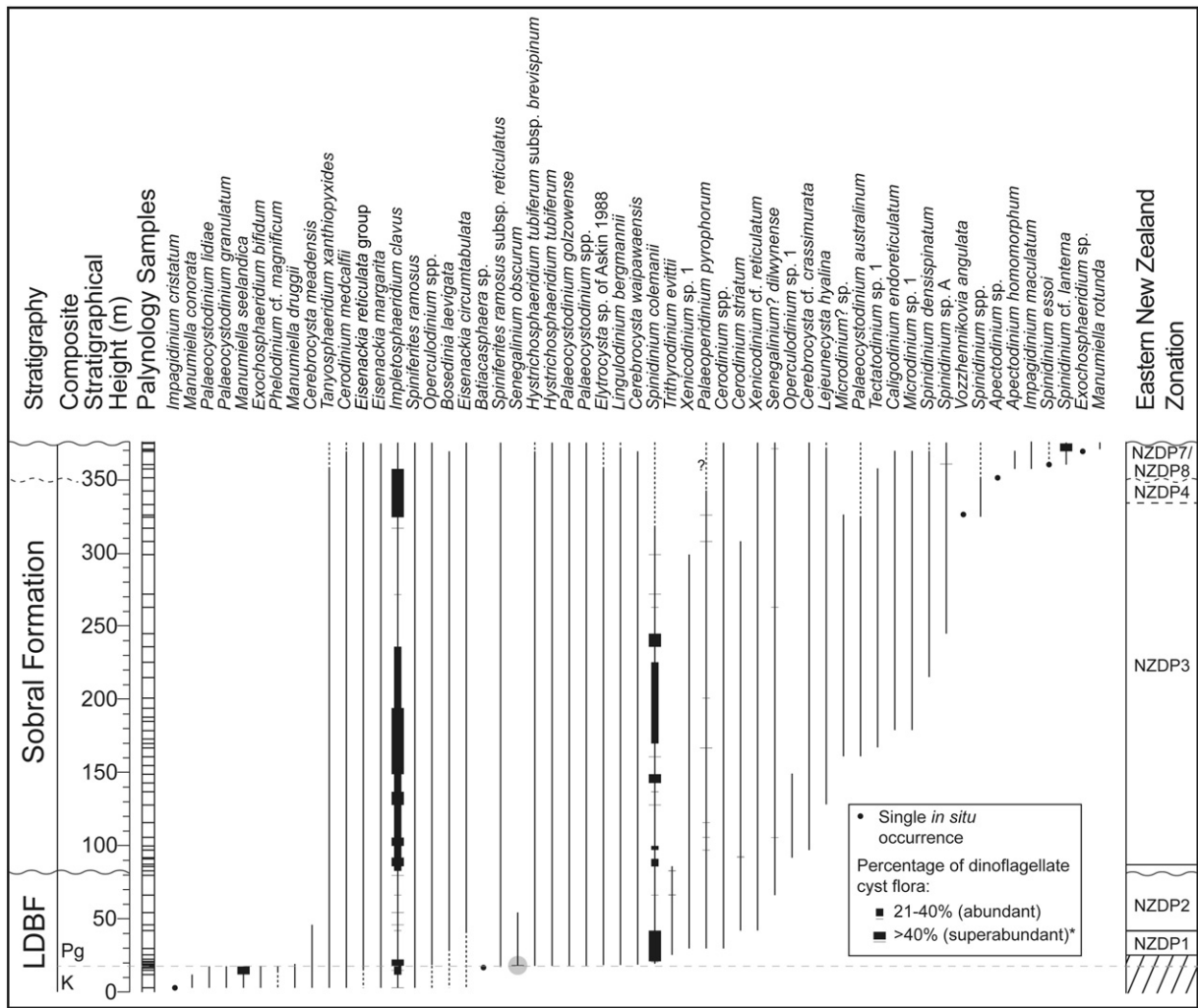


Fig. 4. Dinoflagellate cyst range chart for section D9.605; uppermost López de Bertodano Formation (LDBF) and overlying Sobral Formation. Presumed reworked occurrences are not included, these are in Supplementary Table 1. Taxa are plotted in order of their lowest, then highest occurrences. The base and top of some ranges are extended with a dashed line to include data from previous work on the Seymour Island succession (Askin, 1988a; Wrenn and Hart, 1988; Bowman et al., 2012). *Eisenackia reticulata* and *Cassidium fragile*, two similar reticulate gonyaulacoid taxa, are considered together as the “*Eisenackia reticulata* group” following the approach of Crouch et al. (2014). Horizontal bars mark horizons or intervals where certain taxa are abundant or superabundant; the grey circle highlights the abundance acme of *Senegalinium obscurum* that helps identify the K–Pg boundary on Seymour Island. Dashed wavy line represents the presence of an inferred hiatus discussed herein. Correlation with the New Zealand dinoflagellate zonation scheme for the Paleocene (Crouch et al., 2014) is also plotted and discussed in the text.

(Fig. 4; Thorn et al., 2009; Bowman et al., 2012). This zone extends to ~1.45 m above the K–Pg boundary on Seymour Island because the top is defined by the HO of *Manumiella druggii* (Fig. 6; Wilson, 1984, 1987; Bowman et al., 2012; Fig. 6). Bowman et al. (2012) determined that this species was restricted to the Maastrichtian in section D5.251, but this is likely due to lower resolution sampling across this interval. *Manumiella druggii* has also been recorded from the earliest Paleocene in other K–Pg boundary sections worldwide (e.g. Hultberg, 1986; Willumsen, 2010).

At 18.0 m in D9.605, the dinoflagellate cyst *Senegalinium obscurum* appears abruptly in high numbers (23% of the dinoflagellate cysts; Figs. 3, 4). Askin (1988b) and Elliot et al. (1994) identified a *Senegalinium obscurum* abundance acme as marking the K–Pg boundary, together with other biostratigraphical evidence and an iridium anomaly. This event identifies the K–Pg boundary in all coeval sections on Seymour Island (Askin and Jacobson, 1996; Bowman et al., 2012). Askin and Jacobson (1996) discussed in detail the factors potentially affecting the record of dinoflagellate cysts across the K–Pg transition on Seymour Island. They concluded that none prevent the identification of the boundary or interpretation of environmental trends. *Senegalinium obscurum* is cosmopolitan and is present across the K–Pg

boundary in the highest northern latitude K–Pg section at Nuussuaq, Greenland (Dam et al., 1998) and in Tunisia (M’Hamdi et al., 2013), but no mention is made of an acme at either of these sites. The LO of *Senegalinium obscurum* occurs within two overlapping sub-sections (D9.600 and D9.601) of composite section D9.605 near the base of a glaucony-rich unit (Fig. 2, Supplementary Table 1). Considering the stratigraphical level of this significant bioevent with respect to sampling resolution in both sub-sections the nominal K–Pg boundary is placed at 17.85 m in D9.605 (Fig. 2, illustrated in Supplementary Fig. 1).

Of the twenty dinoflagellate cyst taxa present in the uppermost Maastrichtian (including those recorded in Bowman et al., 2012), only six appear to have their HO coincident with the K–Pg boundary. These are *Exochosphaeridium bifidum*, *Palaeocystodinium granulatum*, *Palaeocystodinium lidiae*, *Phelodinium cf. magnificum* and, most notably, *Manumiella seelandica*, which is superabundant just prior to this level (Fig. 4). *Isabelidinium* spp. were also recorded up to the K–Pg boundary by Bowman et al. (2012), but were not found in D9.605.

To further support the placement of the K–Pg boundary using dinoflagellate cysts, rare specimens of *Carpatella cornuta* and *Damassadinium californicum* were observed immediately above an iridium anomaly in a parallel section on Seymour Island (Elliot et al., 1994; Askin and

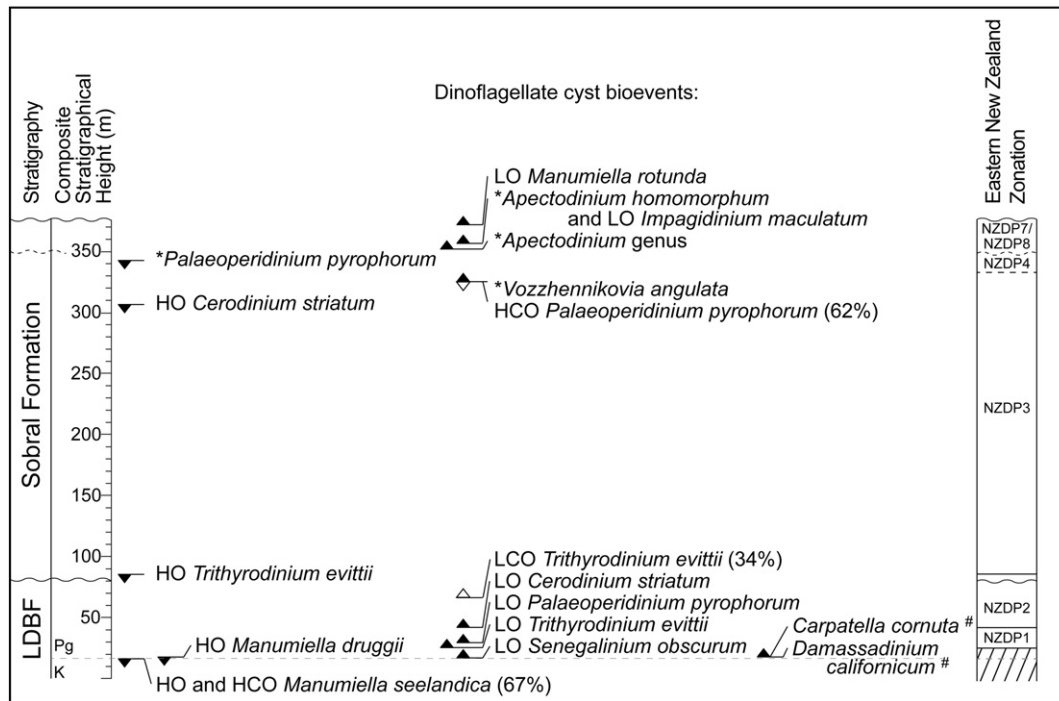


Fig. 5. Significant dinoflagellate cyst bioevents within the uppermost Lópe de Bertodano Formation (LDBF) and the overlying Sobral Formation, section D9.605. #, dinoflagellate cyst taxa recorded by Elliot et al. (1994) from a parallel section. *, bioevents that are not necessarily range bases or tops due to the rarity of specimens, the presence of an inferred hiatus (dashed wavy line) or proximity to the top of the section. LO, lowest occurrence; LCO, lowest common occurrence; HO, highest occurrence; HCO, highest common occurrence. Correlation with the New Zealand dinoflagellate zonation scheme for the Paleocene (Crouch et al., 2014) is also plotted and discussed in the text.

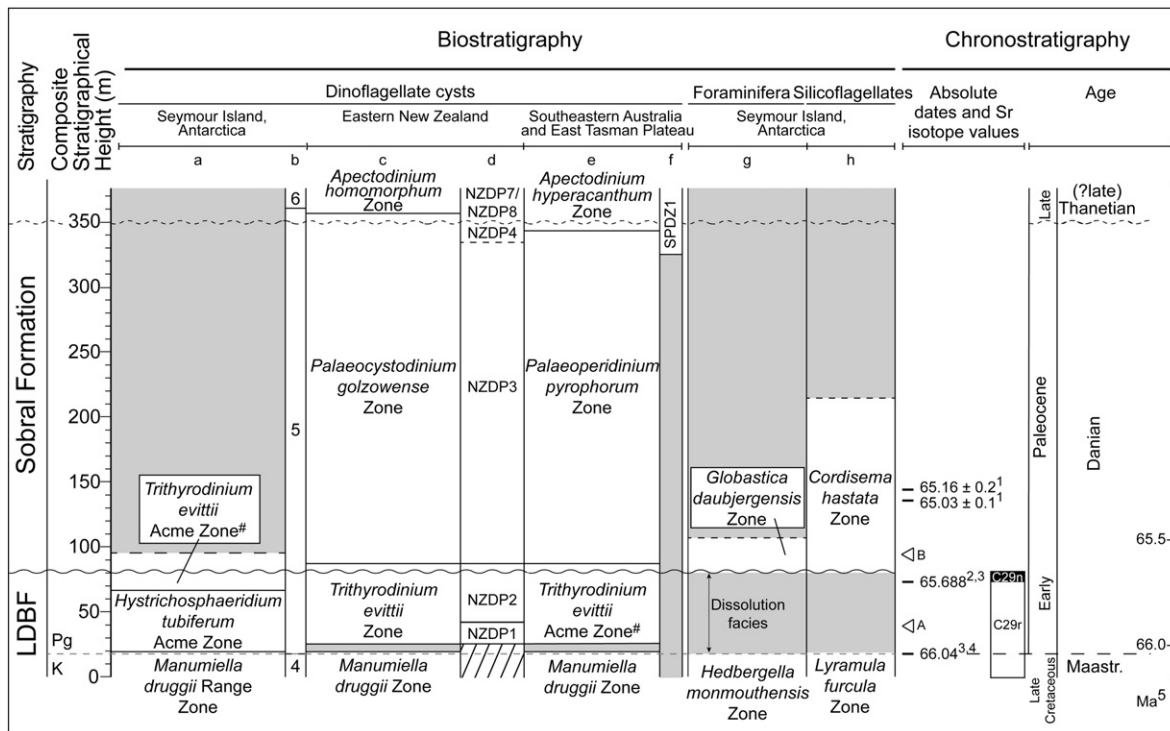


Fig. 6. Composite age model for the uppermost Lópe de Bertodano Formation (LDBF) and the overlying Sobral Formation, section D9.605. Solid wavy line at ~80 m represents the sharp formational contact, minimal hiatus inferred. Dashed wavy line at ~350 m represents the inferred hiatus discussed herein, no contact observed (gully in the field). Biostratigraphy after: a, Bowman et al. (2012; top of *Trithyrodinium evittii* Acme Zone unseen in section D5.251); b, Askin (1988a); c, Wilson (1984, 1987, 1988); d, Crouch et al. (2014); e, Partridge (2006); f, Bijl et al. (2013); g, Huber (1988); h, Harwood (1988). #, after Helby et al. (1987). Strontium isotope values (McArthur et al., 1998): Arrow A, gastropod, 21 m (above K–Pg boundary), $^{87}\text{Sr}/^{86}\text{Sr} = 0.707802$; Arrow B, *Cucullaea ellioti*, 76 m, $^{87}\text{Sr}/^{86}\text{Sr} = 0.707833$. ¹, U–Pb zircon dates from airfall tuff beds (Condon): D9.085.1 at 136.8 m, D9.087.1 at 142.8 m (D9.605); ², palaeomagnetic analysis along strike from section D9.605, uppermost LDBF correlates to the base of C29n (Tobin et al., 2012; refer to Bowman et al. (2013a) for section correlation); ³, chronostratigraphy after Gradstein et al. (2012); ⁴, K–Pg boundary identified by dinoflagellate cyst biostratigraphy and an iridium anomaly from a parallel section (Elliot et al., 1994; Bowman et al., 2012); ⁵, timescale based on absolute dates and magnetostratigraphically-calibrated dinoflagellate cyst bioevents in the southern mid to high palaeolatitudes (see text). The final ammonite zone of the Maastrichtian is the *Pachydiscus ultimus* zone (Witts et al., 2015 and references therein).

Jacobson, 1996). Although these taxa were not recorded from section D9.605, they are important biostratigraphical markers, ranging from the K–Pg boundary to the latest Danian (*Carpatella cornuta*) and earliest Thanetian (*Damassadinium californicum*) (e.g. Hansen, 1977; Powell, 1992; Stover et al., 1996; Willumsen, 2004; Açıkalin et al., 2015). Willumsen (2004, 2010) recorded the LO of *Carpatella cornuta* (along with other *Carpatella* species) in samples immediately above the K–Pg boundary in New Zealand.

Against a background of gradual dinoflagellate cyst diversification leading up to the K–Pg boundary (Bowman et al., 2012, 2013a), the apparent rate of inception immediately following the K–Pg event did increase, although numbers of new taxa were still relatively few (Fig. 4). It is notable that the K–Pg boundary beds are glaucony-rich, suggesting a period of slower sedimentation (Macellari, 1988), though as noted earlier an autochthonous origin for the glaucony is yet to be documented. If the boundary beds are condensed, however, it is possible that the actual LOs of the earliest Danian taxa may not have been isochronous at the K–Pg boundary, but this is unresolvable at the sampling resolution herein.

Bowman et al. (2012) correlated dinoflagellate cyst biozones 1 to 5 of Askin (1988a) to the Maastrichtian to earliest Danian of section D5.251. Zones 4 to 6 of Askin (1988a) can now be correlated to section D9.605 (Fig. 6). Zone 4 correlates to the lowermost part of section D9.605, up to the LO of *Senegalinium obscurum*, approximately coincident with the K–Pg boundary.

4.2. Danian

Twelve species survived the K–Pg event including the thereafter short-lived *Cerebrocysta meadensis* and *Manumiella druggii* (Fig. 4). *Bosedinia laevigata*, *Eisenackia circumtabulata* and *Operculodinium* spp. were not recorded below the K–Pg boundary in section D9.605, but are known to occur in Maastrichtian sediments lower in the succession (Askin, 1988a; Bowman et al., 2012). Nine taxa have their lowest occurrences at or immediately above the K–Pg boundary. Up section, all of these new taxa, except *Senegalinium obscurum*, are stratigraphically long-ranging and occur throughout the rest of the López de Bertodano and Sobral formations. Above this initial radiation, several more taxa have LOs all within ~25 m of the K–Pg boundary, notably *Trithyrodinium evittii*, *Palaeoperidinium pyrophorum* and *Cerodinium striatum* (Figs. 3, 4, 5).

In the lowermost Danian, the *Hystrichosphaeridium tubiferum* Acme Zone defined by Bowman et al. (2012) occurs between 19.3 (the HO of *Manumiella druggii*) and 66.3 m (the lowest common occurrence (LCO) of *Trithyrodinium evittii*) in D9.605 (Figs. 5, 6). The short-lived *Hystrichosphaeridium tubiferum* acme recorded in the D5.251 section was not observed in section D9.605, possibly because it occurred between sampled horizons.

Crouch et al. (2014) defined the LO of *Trithyrodinium evittii* as the base of the revised Paleocene dinoflagellate cyst zonation for New Zealand (the base of NZDP1), rather than the first consistent appearance datum used in Australia (Helby et al., 1987, fig. 40). Drugg (1967) stated that *Trithyrodinium evittii*, a cosmopolitan taxon, is restricted to the Danian at its type locality in California. It appears to have had low-latitude affinities (e.g. Vellekoop et al., 2015), but it is also present in the Maastrichtian in the high northern palaeolatitudes (Pedersen and Nøhr-Hansen, 2014).

The base of NZDP1 in New Zealand is coincident with the K–Pg boundary (Crouch et al., 2014). However, on Seymour Island *Trithyrodinium evittii* has its LO ~7.6 m above the K–Pg boundary (Figs. 4, 5). The acme of *Senegalinium obscurum* on Seymour Island is not seen in New Zealand, which may be facies-controlled or absent due to a short-lived hiatus in some sections (Hollis, 2003). Furthermore, the HO of *Manumiella druggii* occurs within NZDP1 in New Zealand, which in the Seymour Island section occurs below the LO of *Trithyrodinium evittii* (Fig. 5). The top of NZDP1 is defined in New

Zealand as the LO of *Cerodinium striatum* (Crouch et al., 2014). On Seymour Island, this defines the equivalent of the top of this zone at 42.0 m in D9.605 (Figs. 5, 6).

NZDP1 correlates to the lower part of Zone 5 of Askin (1988a) on Seymour Island, which dominates the current section D9.605 (Fig. 6). The base of Askin's (1988a) Zone 5 is defined as the LO of *Senegalinium obscurum*. However, the top was not precisely defined, but was illustrated at the LO of *Spinidinium* cf. *lanterna* and the HO of *Palaeoperidinium pyrophorum* (Askin, 1988a, Fig. 6).

The interval from 42.0 m to 85.8 m in section D9.605 correlates with NZDP2, between the LO of *Cerodinium striatum* and the HO of *Trithyrodinium evittii*. This zone crosses the López de Bertodano/Sobral formational boundary, across which there is no appreciable change in the dinoflagellate cyst flora. The top of NZDP2 correlates with the top of the *Trithyrodinium evittii* Zone of Wilson (1987, 1988) (Figs. 5, 6).

The overlying NZDP3 is characterised in New Zealand by frequent to abundant *Palaeoperidinium pyrophorum* with the decrease from the HCO of this taxon to rare specimens within the top of this zone (Crouch et al., 2014, fig. 14). The base of NZDP3 in the Sobral Formation is well constrained at the HO of *Trithyrodinium evittii* at 85.8 m followed by persistent *Palaeoperidinium pyrophorum*, at intervals occurring in high numbers (Supplementary Table 1). However, defining the equivalent of the top of NZDP3 on Seymour Island is uncertain due to the absence of *Senoniasphaera inornata* in D9.605. We tentatively correlate the NZDP3/NZDP4 boundary with ~333 m in D9.605, which incorporates the abrupt decline in abundance of *Palaeoperidinium pyrophorum* near the top of this zone (Figs. 5, 6). Crouch et al. (2014) also noted that the LO of *Vozzhennikovia angulata* occurs within NZDP3, which is consistent with rare specimens at ~325 m in D9.605 (Fig. 5). The top of NZDP4 in New Zealand is defined by the LO of *Deflandrea foveolata*, but in the absence of this taxon, the HO of *Palaeoperidinium pyrophorum* can be used as a marker (Crouch et al., 2014). We consider the last *in situ* *Palaeoperidinium pyrophorum* to be at 342.3 m, and therefore tentatively place the top of NZDP4 between here and the next sample at 351.3 m.

Throughout section D9.605, the influence of changing depositional settings appears to have had a minimal effect on species turnover. For example, the dinoflagellate cyst floras across the López de Bertodano/Sobral formational boundary in D9.605 are relatively unaffected despite significant downcutting seen laterally along this contact (e.g. Sadler, 1988; Olivero, 2012) (Fig. 4). Higher in the Sobral Formation, *Microdinium?* sp., *Palaeocystodinium australinum* and *Tectatodinium* sp. 1, have their LOs within the glauconitic interval at ~160–175 m in D9.605 (Figs. 2, 4), perhaps reflecting the condensation that is suggested by the concentration of autochthonous glaucony at this level. If the glaucony is *in situ* at this level, this may suggest slight condensation. However, the trend of gradually incoming species throughout this part of the sequence was not disrupted (Fig. 4). In addition, a slight turnover at ~325 m is coincident with the observation of concentric concretionary pillars within delta front sands and single occurrences of *Thyasira townsendi* and a lucinid bivalve. This perhaps indicates the onset of marine seep activity (Little et al., 2015).

Zones NZDP1 to NZDP4 are all dated as Danian in New Zealand implying that the uppermost López de Bertodano Formation (Unit 10) and the majority of the Sobral Formation are Danian in age (Fig. 6), as originally suggested by Askin (1988a). Correlation of the *Trithyrodinium evittii* Acme Zone and *Palaeoperidinium pyrophorum* Zone of Partridge (2006) from the Gippsland Basin, southeastern Australia supports this interpretation (Fig. 6).

In addition, silicoflagellate and foraminifera biostratigraphy supports a Danian age up to at least ~210 m in D9.605 (Harwood, 1988; Huber, 1988; Fig. 6). Harwood (1988) presents diatom and silicoflagellate data up to ~110 m into the Sobral Formation on his section line (top of sampling interval T7, Fig. 2). Using lithological correlation, and data presented in Huber (1988), this is equivalent to ~210 m in D9.605; midway through the Sobral Formation (Fig. 2, Supplementary Methodology).

Harwood (1988) also stated that characteristic Late Paleocene diatoms (e.g. *Hemiaulus incurvus*) and silicoflagellates (e.g. *Naviculopsis* spp.) are absent for at least the lower 250 m of the Sobral Formation (up to ~330 m in D9.605).

4.3. Late Paleocene

At 351.3 m, there is a significant event in the marine palynoflora in D9.605 with the LO of the genus *Apectodinium* and just above the appearance of *Apectodinium homomorphum* at ~357.3 m (Figs. 3, 4, 5). These rare, but well-preserved specimens from the uppermost Sobral Formation record the earliest *in situ* occurrence of this subfamily from Antarctica. However, *Apectodinium homomorphum* is relatively rare in section D9.605.

The earliest global appearance of the genus *Apectodinium* is in low latitudes of the Tethys during the mid Paleocene (Crouch et al., 2003a, 2014). In New Zealand, Crouch et al. (2014) first recorded *Apectodinium homomorphum* (included within their “*Apectodinium* round group”) within the uppermost NZDP8 biozone in the latest Paleocene. The LO is known to be within international nannofossil Zone NP9 and close to the Paleocene–Eocene boundary (Crouch et al., 2014, fig. 14). *Apectodinium homomorphum* occurs in very low abundances from 624 mbsf (metres below sea floor) at ODP Site 1172 during the late Thanetian (Bijl et al., 2013). However, the base of their lowest zone SPDZ1 was defined using the HCO of *Palaeoperidinium pyrrophorum*, which occurs at ~324 m in D9.605 (Fig. 5; Bijl et al., 2013). On the East Tasman Plateau, zone SPDZ1 extends up to immediately prior to the Paleocene–Eocene boundary, coincident with the LCO of *Apectodinium homomorphum* (Bijl et al., 2013). *Apectodinium* specimens are rare in section D9.605. Notably, as on Seymour Island, *Eisenackia reticulata* co-occurs with *Apectodinium homomorphum* in ODP Site 1172 (Bijl et al., 2013). In the Gippsland Basin of Australia, the LOs of *Apectodinium homomorphum* and *Apectodinium hyperacanthum* define the base of the *Apectodinium hyperacanthum* Zone. This is also within nannofossil zone NP9 during the latest Thanetian (Partridge, 2006; Fig. 6). The sequence of bioevents within the upper Sobral Formation is complex allowing slightly different biostratigraphical interpretations. Firstly, if the *Apectodinium* specimens are indicative of the uppermost part of NZDP8 as they are in New Zealand, then the uppermost Sobral Formation (from 351.3 m) is all latest Paleocene in age.

In New Zealand, the LO of *Manumiella rotunda* and the higher LO of *Apectodinium* are significant bioevents in the Late Paleocene (Crouch et al., 2014). The LO of *Manumiella rotunda* occurs within the upper levels of NZDP7 in New Zealand and it is recorded by Wilson (1988) up to the Paleocene–Eocene boundary, overlapping with the incoming of *Apectodinium* in the latest Paleocene. Both *Manumiella rotunda* and specimens of *Apectodinium* are present, but rare in the uppermost Sobral Formation, but in contrast to the New Zealand record, the LO of the genus *Apectodinium* (at 351.3 m) is lower than the LO of *Manumiella rotunda* (at 370.8 m; Figs. 4, 5). This biostratigraphical conundrum may suggest a reversal in the stratigraphy, particularly as the *Apectodinium* specimens occur within a discrete interval (351.3–369.3 m) prior to the first record of *Manumiella rotunda*. However, the intervening bed boundary at 370.3 m is gradational and clearly not erosional. Further, there is no evidence of major synsedimentary disturbance in the upper Sobral Formation (for example, slumping or exotic slide blocks) that could have inverted the succession. Alternatively, this apparently delayed appearance of *Manumiella rotunda* may be facies-related. The abrupt dominance of *Spinidinium* cf. *lanterna* in the uppermost Sobral Formation (from 369.3 m) suggests that the depositional setting had changed in these uppermost beds; defined as a separate zone (Zone 6) by Askin (1988a).

If the upper Sobral Formation from 351.3 m is latest Paleocene in age, this would require the well-preserved specimens of *Eisenackia margarita* and *Eisenackia reticulata* in the uppermost part of the section to be reworked, as their LO is the top of NZDP7 in New Zealand. Two specimens of *Vozzhennikovia angulata* (Fig. 3; 360.3 m) may also be reworked from

lower in the succession as their HO in New Zealand is at the top of NZDP5. Reworking of palynomorphs is certainly possible within the shallow marine fan-delta setting interpreted for the upper part of the formation (unpublished data). However, alternatively, the HO of these taxa may be heterogeneous across the mid to high southern palaeolatitudes, perhaps due to varying depositional settings, and occur later in Antarctica than New Zealand.

The consistent presence of *Impagidinium maculatum* also supports a latest Paleocene interpretation for the top of the Sobral Formation, which occurs rarely from NZDP4 but consistently throughout NZDP7 and 8 in New Zealand (mid-Waipara River sections and the Toi Flat-1 core; Crouch et al., 2014). Wilson (1988) also noted that the LO of *Apectodinium homomorphum* and *Impagidinium maculatum* was coincident (comparable to the record in D9.605) in the latest Paleocene of New Zealand. With the HO of *Palaeoperidinium pyrrophorum* marking the top of NZDP4 in this section at 342.3 m, this interpretation means that zones NZDP5, 6 and 7 are absent in the succession. With the appearance of *Apectodinium* at 351.3 m, this suggests that the remainder of the section could be equivalent to uppermost NZDP8.

An alternative biostratigraphical interpretation is that the well-preserved specimens of *Eisenackia margarita* and *Eisenackia reticulata* at the top of the section are *in situ*. They may be very near to the top of their range with the LO of *Manumiella rotunda* (370.8 m) immediately prior to their HO, as recorded in New Zealand in uppermost NZDP7 (Crouch et al., 2014). This would require a much earlier appearance of *Apectodinium* in Antarctica than in New Zealand or the East Tasman Plateau (Bijl et al., 2013; Crouch et al., 2014), perhaps as early as the latest Selandian. This interpretation implies that only NZDP5 and NZDP6 are missing in the succession between the HO of *Palaeoperidinium pyrrophorum* at 342.3 m and the LO of *Apectodinium* at 351.3 m. In support of this interpretation, Hollis et al. (2014) refined the age of the LO of *Manumiella rotunda* in New Zealand to 59.3 Ma (latest Selandian), although as previously mentioned, it is rarely found and its LO may be heterogeneous across mid to high southern palaeolatitudes. However, the earliest appearance of *Apectodinium homomorphum* is in the low latitudes of the Tethys during the mid Paleocene (Crouch et al., 2003a, 2014) and it is difficult to explain how it could have appeared in the Antarctic prior to the mid latitudes of New Zealand, the East Tasman Plateau and southeastern Australia.

Assemblages dominated by *Apectodinium* tend to be correlated to intervals of high sea surface temperature or nutrient levels, for example, at the Paleocene–Eocene Thermal Maximum (PETM) at ~56 Ma (Crouch et al., 2001, 2003b; Bijl et al., 2011, 2013; Crouch et al., 2014). It is probable that even the few *Apectodinium* specimens from Seymour Island are likely to have been related to regional warming, particularly as their appearance coincides with a significance decrease in *Impletosphaeridium clavus* (Fig. 4, Supplementary Table 1). *Impletosphaeridium clavus* has been previously related to particularly cold intervals during the Maastrichtian (Bowman et al., 2013a,b). Further investigation of palaeoclimatic trends in the Antarctic Peninsula region during the Paleocene awaits more comprehensive analysis of the marine and terrestrial palynology of this succession. The presence of even rare specimens of *Apectodinium homomorphum*, however, suggests that sediments recording the PETM may yet be found if future drilling targets the eastern part of the depositional basin in the Weddell Sea beyond Seymour Island.

To corroborate the results from the upper part of D9.605, pilot samples have been processed for palynomorphs from another exposure of the uppermost Sobral Formation at Cape Wiman in the north of Seymour Island (Fig. 1). These coarser samples contain fewer, less well-preserved palynomorphs, but similar dinoflagellate cyst assemblages to those seen in D9.605. However, neither of the key marker taxa (*Apectodinium homomorphum* or *Manumiella rotunda*) were recorded in this initial study. Therefore, we recognize that the correlation based on dinoflagellate cysts for the upper part of the Sobral Formation must remain tentative until additional evidence becomes available.

Both the alternative biostratigraphical interpretations for the uppermost Sobral Formation of D9.605 imply that between the HO of *Palaeoperidinium pyrophorum* at 342.3 m and the LO of *Apectodinium* at 351.3 m in D9.605, the latest Danian, Selandian and possibly early Thanetian are either significantly condensed, or missing at an inferred hiatus (Fig. 6). Given the lack of sedimentary evidence for a significantly condensed sequence during this interval, we consider a hiatus to be more likely (Fig. 2). It is possible that the true HO of *Palaeoperidinium pyrophorum* may have been higher than recorded, and the true LO of *Apectodinium homomorphum* lower than recorded, both lost in the hiatus. In the field, this critical interval (~345–350 m) is mainly scree-covered and no erosional/hiatal surface was identified. However, a marked change in sedimentary provenance is evident at ~350 m, where we tentatively place the unconformity, from quartz-rich sands to sands enriched in volcanic grains (Fig. 2). Discrete volcanic pebbles and granules become prominent above this level.

At Cape Wiman, in northern Seymour Island, a preliminary sedimentological study suggests that a comparable provenance change occurs at a stratigraphical level coincident with the last abundant *Palaeoperidinium pyrophorum*. Other workers have referred these strata (~350–376 m in D9.605), partly or wholly, to the Upper Paleocene Cross Valley Formation (Montes et al., 2010; Marensi et al., 2012). Although acknowledging some lithological and stratigraphical similarities, facies comparisons and preliminary palynological data are considered here to support continued assignment to the Sobral Formation. Potential resolution of this ambiguity must await the completion of this ongoing palynological work on the Cross Valley Formation.

5. Chronostratigraphy

Magnetic polarity zonal boundaries were correlated to D9.605 with the K–Pg boundary and the López de Bertodano/Sobral formational boundary as tie-points (Tobin et al., 2012; Bowman et al., 2013a). Magnetostratigraphy is not available for the Sobral Formation, but existing data from Tobin et al. (2012) provides time constraints for the lower ~180 m of D9.605 (Fig. 6). In addition, strontium isotope ($^{87}\text{Sr}/^{86}\text{Sr}$) values from bivalves and gastropods from Unit 10 of the López de Bertodano and throughout the Sobral Formation support a Paleocene age (McArthur et al., 1998; Fig. 6). However, a global compilation of strontium isotope values shows little variation during this time interval, preventing further refinement of the dating (McArthur et al., 2012).

Dating of zircons using U–Pb geochronology from section D9.605 has also been undertaken on samples from two ash beds in the lower Sobral Formation at 136.8 m (D9.085.1) and 142.8 m (D9.087.1) (Fig. 6). The youngest of these grains were then processed further for more precise age determinations. Sample D9.087.1 yielded a mixed morphological population, which was subject to screening by laser ablation ICP-MS. This indicated a mix of Jurassic and Cretaceous dates with a subordinate population yielding late Cretaceous to early Paleogene dates. These late Cretaceous to early Paleogene zircons were extracted for CA-ID-TIMS analyses and the results are presented in Supplementary Table 2 and Supplementary Fig. 2. The CA-ID-TIMS analyses of zircon from D9.087.1 yielded a coherent population with a weighted mean $^{206}\text{Pb}/^{238}\text{U}$ date of $65.25 \pm 0.10/0.10/0.13$ (MSWD = 0.99, $n = 6$, z11, z12, z15, z20, z24 and z26). The CA-ID-TIMS analyses of zircon from D9.085.1 yielded a coherent population with a weighted mean $^{206}\text{Pb}/^{238}\text{U}$ date of $65.032 \pm 0.085/0.087/0.121$ (MSWD = 0.29, $n = 4$, z8, z9, z10, z21). The interpreted dates based upon the coherent population of youngest dates for these two samples are in reverse stratigraphical order and do not overlap at the 2σ level. An alternative interpretation for D9.087.1 can be made where a subset of the youngest dates is chosen to base the age of the ash bed on, assuming that some of the older dates are based upon zircons that contain significant portions that pre-date eruption. For example choosing the youngest five of the six gives a weighted mean $^{206}\text{Pb}/^{238}\text{U}$ date of $65.16 \pm 0.15/$

$0.15/0.17$ of (MSWD = 0.54, $n = 5$, z11, z12, z15, z20 and z24), which is indistinguishable from the date for the underlying sample D9.085.1. Combined, these data indicate a numerical age of $\sim 65.05 \pm 0.15$ Ma (total uncertainty) for the Sobral Formation at a level of ~140 m.

A best-fit age model for D9.605, based on the biostratigraphical and chronostratigraphical evidence discussed herein, is presented in Fig. 6. Linear interpolation has been used between the known ages of the K–Pg boundary and magnetostratigraphical reversal boundaries based on Gradstein et al. (2012) and Tobin et al. (2012). This is supplemented by U–Pb ages (this study) and strontium isotope values (McArthur et al., 1998). The timescale for the lower ~150 m of D9.605 is well constrained, but is uncertain above the levels of the U–Pb ages.

6. Palaeogeographical implications

Mid to high palaeolatitude dinoflagellate cyst assemblages of Maastrichtian to Late Paleocene age were similar in composition throughout the Southern Ocean. This implies that unrestricted marine connections were present either around the Antarctic margin, or through the continental interior, during final Gondwana fragmentation. The following discussion outlines the geological evidence relating to the tectonic development of these marine pathways and whether current interpretations of Antarctic palaeotopography and ocean circulation models agree with this fossil evidence.

Seymour Island, at the tip of the Antarctic Peninsula, forms the northernmost extent of West Antarctica. This region is comprised of several tectonic blocks along the palaeo-Pacific margin of Gondwana (Vaughan and Pankhurst, 2008; Michaux, 2009; Fig. 7). This is a critical region for investigating how the palaeotopography and the fragmentation dynamics of this sector of Gondwana can inform understanding of south polar palaeobiogeography and palaeoclimate.

Bowman et al. (2012) discussed the requirement for a marine connection during the Maastrichtian between the Weddell embayment and the Ross Sea, the boundary zone between West and East Antarctica (Fig. 7). This explained the similarity of dinoflagellate cyst floras from Seymour Island and New Zealand during that time interval, which has been shown herein to extend into the Danian and even the Thanetian. However, does all of the available fossil evidence agree with tectonic reconstructions of Antarctic palaeotopography through this time interval? Furthermore, do the fossil and tectonic evidence combined still support the existence of a latest Cretaceous to Paleocene transAntarctic seaway?

Huber (1988) suggested the existence of a transAntarctic marine connection to explain the circum-Antarctic distribution of foraminifera, based on evidence from latest Cretaceous sediments on Seymour Island. In addition, reworked Cretaceous foraminifera occur in middle Miocene sediments beneath the Ross Ice Shelf and in Quaternary sediments of Taylor Valley (Webb and Neall, 1972; Webb, 1979; Fig. 7). These data suggest marine deposition in the Ross Sea region at this time. In the macrofossil record, all of the ammonite genera and several species recorded from the Maastrichtian of Seymour Island are found in the Haumurian (Campanian–Maastrichtian) of New Zealand (Henderson, 1970). In general, the Antarctic ammonite fauna are similar to those from South America, New Zealand and Australia (Witts et al., 2015).

Gastropod genera from the lower Sobral Formation suggest a relatively strong marine macrofaunal connection with the Danian Wangaloa Formation of New Zealand (Crame, 2013; Crame et al., 2014). The Broken River, Kauru and Abbotsford Formations in New Zealand are all lateral equivalents and host a very similar fauna (Finlay and Marwick, 1937; Beu and Maxwell, 1990; Stilwell, 2003; Stilwell et al., 2004; Beu and Raine, 2009; Crame et al., 2014). There are also four gastropod genera from the same interval of the Sobral Formation that can be compared with taxa in the Danian Cerro Dorotea Formation of southwestern Patagonia (Griffin and Hunicken, 1994; Crame et al., 2014). These are the genera *Heteroterma*, *Pseudotylostoma*, *Austrosphaera* and *Taioma*. Gastropod fauna from northern Patagonia also compare with those of the Wangaloa Formation (del Río, 2012). All these occurrences

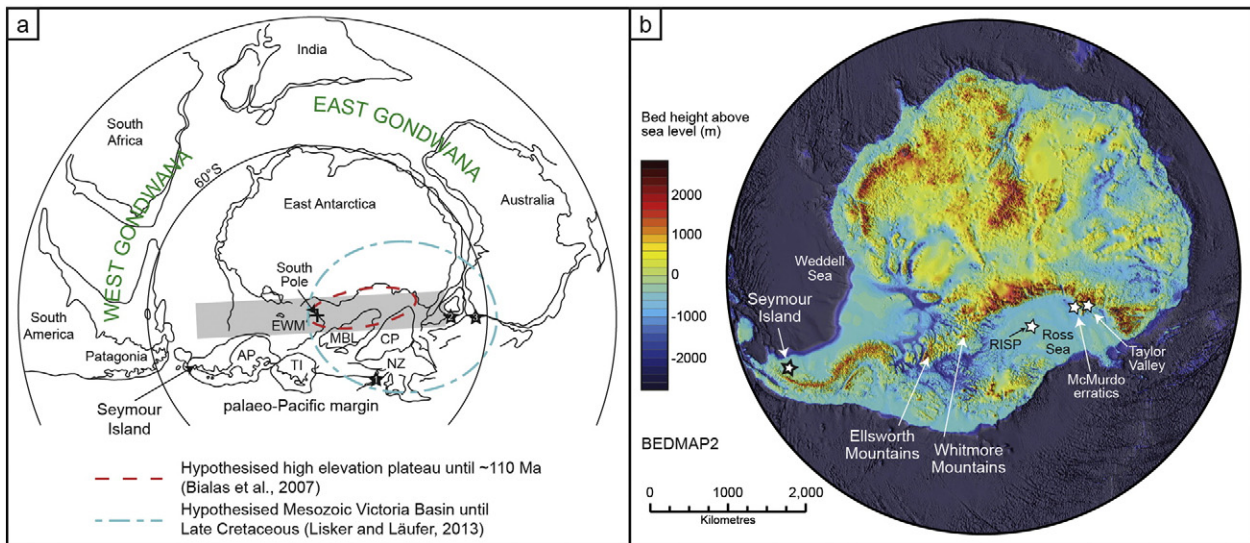


Fig. 7. (a) Reconstruction of the palaeo-Pacific margin of Gondwana ~100 Ma showing the position of the tectonic blocks of West Antarctica and Seymour Island, prior to the separation of Zealandia (after Mukasa and Dalziel, 2000). AP, Antarctic Peninsula; TI, Thurston Island; EWM, Ellsworth–Whitmore Mountains; MBL, Marie Byrd Land; CP, Campbell Plateau; NZ, North and South Islands, New Zealand. Black numbered stars refer to localities discussed in the text – all had drifted further north by the Paleocene with ongoing Gondwana fragmentation: 1, East coast basins, New Zealand (Crouch et al., 2014); 2, East Tasman Plateau, offshore Tasmania (Bijl et al., 2013); 3, Gippsland Basin, southeast Australia (Partridge, 2006). Grey shaded area, West to East Antarctic boundary zone and potential route of a transAntarctic strait. (b) BEDMAP2, bed topography map of Antarctica (Fretwell et al., 2013) to highlight elevated regions and locate fossil records of marine organisms within the Ross Sea of Cretaceous to Paleogene age. RISP, Ross Ice Shelf Project, J-9 cores (e.g. Wrenn and Beckman, 1982); McMurdo erratics, Mt. Discovery and Minna Bluff, McMurdo Sound (e.g. Levy and Harwood, 2000); Taylor Valley, Dry Valleys, TransAntarctic Mountains (Webb and Neall, 1972).

suggest that there was a shallow marine link during the Danian, either along the southern Gondwana margin or through a transAntarctic seaway. This link would have connected the marine communities from Patagonia, the Antarctic Peninsula and New Zealand. Bijl et al. (2011) also proposed the existence of a transAntarctic seaway during the mid to Late Eocene (47–36 Ma). This was based on the distribution of circum-Antarctic endemic dinoflagellate cysts, including reworked late Paleogene marine palynofloras from erratics and Neogene seafloor sediments from the Ross Sea (Wrenn and Beckman, 1982; Levy and Harwood, 2000).

A continuous terrestrial link through West Antarctica was also required during the Late Cretaceous and Paleogene. This included a functional land bridge between the Antarctic Peninsula and Patagonia from the Campanian to the Late Paleocene (Reguero et al., 2014). This allowed land mammals and plants to disperse between South America, West Antarctica and Australia (Case, 1988; Woodburne and Case, 1996; Cantrill and Poole, 2002; Reguero et al., 2013). Therefore, both marine and terrestrial organisms are known to have dispersed across Antarctica between the Late Cretaceous and earliest Paleocene. One proposed solution to account for these routes was a closely spaced archipelago through the boundary zone between West and East Antarctica (Bowman et al., 2012). Traditional palaeotopographical models of the Antarctic interior based on modern sub-ice topography minus ice-loading effects produced a similar palaeogeographical feature (Wilson and Luyendyk, 2009; Wilson et al., 2012).

Reconstruction of the palaeotopography between West and East Antarctica during the latest Cretaceous to Paleocene, however, remains uncertain. The proto-Weddell Sea formed by seafloor spreading during the Middle Jurassic to the Early Cretaceous, 165–130 Ma (Dalziel and Lawver, 2001). Therefore, the Weddell embayment and the back-arc basins along its western margin have existed since final Gondwana fragmentation during the Late Cretaceous, ~100 Ma (Elliot, 2013). The back-arc sediments that now form Seymour Island have remained at approximately the same latitude since this time (~64°S; Lawver et al., 1992; Markwick and Valdes, 2004). The Ellsworth Mountains were uplifted prior to 141 Ma and have retained at least 1.8 km of relief (Fitzgerald and Stump, 1991; Wilson et al., 2012; Fig. 7). Grunow et al. (1991) consider the Ellsworth–Whitmore Mountains block to have been in its present

position since ~110 Ma, suggesting a persistent topographical high, and terrestrial barrier, to the south of the Weddell embayment.

Rifting of up to ~600 km in the Ross embayment began during the Late Cretaceous (~105 Ma) and led to the West Antarctic Rift System (Siddoway, 2008; Elliot, 2013). Uplift and denudation episodes of the Transantarctic Mountains culminated during the Eocene ~55 Ma (Decesari et al., 2007; Elliot, 2013). Contrasting theories about the origins of the Transantarctic Mountains and tectonics of the Ross Sea sector invoke either a Mesozoic highland or a vast intra-Gondwana basin across West Antarctica (Studinger et al., 2004; Bialas et al., 2007; Lisker and Läufer, 2013; Fig. 7).

For the plateau theory, numerical modelling suggests the subsidence and rifting of a high plateau that left the Transantarctic Mountains as remnants of the margin (Studinger et al., 2004; Bialas et al., 2007; Wilson and Luyendyk, 2009; Jordan et al., 2013). This hypothesised plateau may have existed until mid Cretaceous times (~110 Ma; Bialas et al., 2007). This then subsided during the Late Cretaceous and Cenozoic, although still remained above sea level by the latest Paleogene (Wilson and Luyendyk, 2009; Wilson et al., 2012).

In contrast, crustal thinning and extension is proposed to account for the Transantarctic Mountains due to rift flank mechanical uplift at much lower elevations (Davey and Brancolini, 1987; Salvini et al., 1997). A re-evaluation of >500 apatite fission-track ages along the length of the Transantarctic Mountains does not support a high plateau across the Ross Sea sector as it required long-term exhumation rather than sediment accumulation (Lisker and Läufer, 2013). Lisker and Läufer (2013) instead invoke the presence of a vast intra-Gondwana basin during Late Triassic to Late Cretaceous times, perhaps encompassing subaerially exposed lowlands and shallow seas (the Mesozoic Victoria Basin; Fig. 7). The Transantarctic Mountains would have been uplifted as a consequence of rifting. This basin would have allowed marine communication between East and West Antarctica and, with such a large basin in place during the Mesozoic, there is no need to significantly change the tectonic regime through the Cenozoic to reach the present-day Ross Sea (Huerta and Harry, 2007; Lisker and Läufer, 2013).

Zealandia began to separate from Gondwana and the Campbell Plateau rifted away from West Antarctica at ~83 Ma, as subduction ceased (Larter et al., 2002; Laird and Bradshaw, 2004; Mortimer, 2004;

Bache et al., 2014). This was the final phase of the fragmentation of Gondwana and formed the modern Antarctic continent (Boger, 2011). At the same time, seafloor spreading began in the Tasman Sea (~85 Ma; Gaina et al., 1998; Sutherland, 1999; White et al., 2013; Bache et al., 2014). A marine barrier to terrestrial dispersal was probably present between Antarctica and Australia by 64 Ma as the South Tasman Rise submerged (Woodburne and Case, 1996). By the end of the Paleocene (56 Ma), the sediments that now form the east coast depositional basins of South Island, New Zealand, were located at ~53°S (King et al., 1999; Cande and Stock, 2004; Hollis et al., 2014). Furthermore, by this time, the East Tasman Plateau (ODP Site 1172) was located at a similar palaeolatitude to Seymour Island at ~65°S (Bijl et al., 2013).

Model ocean currents during the Maastrichtian suggest slow surface flow (0–55 mm s⁻¹ at 5 m annual average depth) down the Pacific margin of the Antarctic Peninsula to New Zealand (Hunter, 2009; Katz et al., 2011; Bowman et al., 2012). A shallow water connection is modelled through the proto-Drake Passage flowing eastwards at this time (Hunter, 2009; Bowman et al., 2012). However, details of this inferred current, and flow direction, are uncertain given evidence for a land bridge coupled with a relatively coarse land-sea mask in the model (Hunter, 2009; Reguero et al., 2014). Ocean circulation through the proto-Drake Passage is modelled to flow in the opposite direction during the middle to late Eocene, joining the South Pacific gyre. Currents flow along the Pacific margin of West Antarctica before passing the East Tasman Plateau on the way to Zealandia (Huber et al., 2004; Bijl et al., 2011).

In summary, fossil evidence suggests marine conditions in at least part of the Ross Sea sector from latest Cretaceous to Paleogene times. By this time, either the hypothesised elevated plateau across the proto West Antarctic Rift System would have been collapsing, or the Mesozoic Victoria Basin would have been in place. It remains uncertain whether a marine strait linking the Weddell Sea to the Ross Sea could have breached the persistently high Ellsworth–Whitmore Mountains block as crucial fossil evidence is lacking from this region of the interior of West Antarctica. We suggest that marine and terrestrial dispersal routes crossing Antarctica between South America and New Zealand/Australia could have passed along the palaeo-Pacific margin of Gondwana. The terrestrial routes avoided the loftiest mountains that form physical barriers to both plants and animals. A functional land bridge between the Antarctic Peninsula and Patagonia (Reguero et al., 2014) would have incorporated marine causeways in order to allow uninterrupted marine connections along the southern Gondwana margin.

Fossil and geochemical data suggest that particularly cold climatic intervals occurred at high southern palaeolatitudes during the Maastrichtian (Bowman et al., 2013a, 2014). The possibility of seasonal sea ice at the Antarctic margin implies that there may have been high elevation ice caps at this time (Bowman et al., 2013a; Gao et al., 2015). A high plateau in the region of the West Antarctic Rift System (Studing et al., 2004; Bialas et al., 2007), may have acted as a site for ice cap development. Although the plateau may have been subsiding by this time, much of this region is thought to have remained above sea level at least until the Eocene (Wilson and Luyendyk, 2009). Such high latitude ice caps could help explain significant falls in global sea level during the Maastrichtian (Miller et al., 2008) and even in the Paleocene (Hollis et al., 2014). In contrast, invoking a significant transAntarctic marine connection or large interior basin would have provided a conduit for heat transport to the centre of Antarctica (Lisker and Läufer, 2013). This may have prevented Late Cretaceous terrestrial glaciation in West Antarctica, with local ice caps perhaps restricted to the interior of East Antarctica (Ferraccioli et al., 2011).

7. Conclusions

A key reference section for the latest Cretaceous to Late Paleocene from Seymour Island, Antarctica, is presented with an age model based primarily on dinoflagellate cyst biostratigraphy and U–Pb

dating of zircons. The majority of the section is Danian in age, with the latest Danian, Selandian and possibly early Thanetian considered missing in an inferred hiatus, which is not specifically expressed in the sedimentology.

Dinoflagellate cyst biostratigraphy from the upper López de Bertodano Formation (latest Maastrichtian to early Danian) and Sobral Formation (Danian to Thanetian) is correlated to biozonation schemes from the Paleocene of the mid to high southern palaeolatitudes. This is supported by additional information from the siliceous microfossil and macrofossil record from Seymour Island. Notably, the earliest *in situ* specimens of the genus *Apectodinium* (including *Apectodinium homomorphum*) are recorded from Antarctica; a key Wetzelielloidea taxon characteristic of Late Paleocene strata worldwide.

Dinoflagellate cyst bioevents compare closely with those from the Paleocene of the eastern basins of New Zealand, correlating with zones NZDP1 to NZDP4 through the upper López de Bertodano Formation and most of the Sobral Formation, and NZDP7/NZDP8 in the uppermost Sobral Formation. NZDP5 and 6, and perhaps also NZDP7, are missing depending on the biostratigraphical interpretation for these uppermost beds, which remains tentative.

The palaeobiogeographical implication of this study is that the dispersal of marine and terrestrial organisms between Patagonia and New Zealand/Australia could have occurred along the palaeo-Pacific margin of Gondwana. For a transAntarctic connection, organisms would have needed to breach the persistent topographical high of the Ellsworth–Whitmore Mountains block to the south of the Weddell embayment. Marine organisms would have required an oceanic strait, and terrestrial animals and plants a relatively low altitude pass. This cannot be precluded but requires additional fossil evidence from this central region of Antarctica. Furthermore, we tentatively support the notion of a high plateau in the boundary zone between West and East Antarctica during the Cretaceous, which could have acted as a potential nucleus for high elevation ice caps. This supports evidence from previous work for particularly cold climate intervals recognized globally during the Maastrichtian and in the South Pacific during the Paleocene.

Supplementary data to this article can be found online at <http://dx.doi.org/10.1016/j.gr.2015.10.018>.

Acknowledgements

UK Natural Environment Research Council (NERC) grants NE/I00582X/1 (PALEOPOLAR) and NE/C506399/1 (Antarctic Funding Initiative) funded this research. The authors thank the School of Earth and Environment, University of Leeds, UK, for support and use of their facilities where this work was initiated. The Environmental Change and Evolution programme of The British Antarctic Survey awarded additional funding to Bowman for STRATABUGS palynological software. The authors would like to thank the rest of the PALEOPOLAR team, particularly Stuart Robinson (University of Oxford) and Dave Kemp (University of Aberdeen), for useful discussions. Jette Halskov (GEUS) is thanked for drafting the sedimentological log. The British Antarctic Survey provided field logistics. James B. Riding publishes with the permission of the Executive Director, British Geological Survey (NERC), Jon R. Ineson with the permission of the Geological Survey of Denmark and Greenland (GEUS). We would also like to warmly thank Chris Hollis and Erica Crouch (GNS Science, New Zealand), and an additional anonymous reviewer, whose constructive comments significantly improved the manuscript.

Appendix A

Taxonomic list of dinoflagellate cysts recorded during this study from the uppermost López de Bertodano Formation and Sobral Formation. ^{rw} Reworked. Author references prior to 2004 listed in Fensome and Williams (2004).

Apectodinium homomorphum (Deflandre & Cookson 1955) Lentin & Williams 1977 emend. Harland 1979

Remarks: Wrenn and Beckman (1982) listed, but did not illustrate, *Apectodinium homomorphum* from a reworked Paleogene palynoflora within the Ross Ice Shelf Project (RISP) J-9 composite core. Levy and Harwood (2000) noted that this was the first published occurrence of the Wetzelielloidea from Antarctica, but the record is not *in situ*.

Apectodinium sp.

Remarks: The single specimen observed (Fig. 3) has an irregular granular surface texture.

Batiacasphaera sp.

Bosedinia laevigata (Jiabo 1978 ex He Chengquan & Qian Zeshu 1979) He Chengquan 1984

Caligodinium endoreticulum Stover & Hardenbol 1994

Remarks: Well-preserved specimens of typically ovoid cysts with a polar archeopyle and microreticulate ornamentation, no horn development and with an irregular calyptra were recovered from the Sobral Formation. Size range of autocyst: 50 (56) 65 µm. Despite microreticulate cyst ornamentation being a feature of *Caligodinium aceras* (Manum & Cookson 1964) Lentin & Williams 1973, a widely distributed member of this genus (Manum and Williams, 1995), these specimens from the Sobral Formation are smaller, and therefore are identified as *Caligodinium endoreticulatum*. Stover and Hardenbol (1994) report this taxon from the Rupelian of Belgium; this Antarctic occurrence extends its stratigraphical range back to the Danian. The genus *Caligodinium* Drugg 1970 emend. Manum & Williams 1995 is known from the James Ross Basin from the Coniacian–early Santonian of the Hidden Lake Formation of Brandy Bay, James Ross Island (*Caligodinium aceras*, Barreda et al., 1999). Willumsen (2010) noted a single specimen of *Caligodinium amiculum* Drugg 1970 (unillustrated) from the Paleocene *Palaeocystodinium golzowense* Zone of the Branch Stream section, Clarence Valley, New Zealand.

^{rw} *Carpatella* sp.

Cassidium fragile (Harris 1965) Drugg, 1967

Remarks: See *Eisenackia reticulata*.

Cerebrocysta cf. *crassimurata* (Wilson, 1988) Fensome et al. (2009)

Remarks: We adopt the approach of Crouch et al. (2014) who prefer to use the genus *Cerebrocysta* for all specimens previously assigned to *Pyxidopsis* Habib 1976, after Fensome et al. (2009). Specimens of *Cerebrocysta* cf. *crassimurata* observed herein have a generally finer macroreticulum with narrower lumina than the type material of Wilson (1988).

Cerebrocysta meadensis (Willumsen, 2010) Fensome et al. (2009)

Remarks: Specimens identified as *Operculodinium* spp. in samples close to the K–Pg boundary in Bowman et al. (2012) may be referable to *Cerebrocysta meadensis*. Isolated archeopyles were also noted in the current study, which are quite distinctive for this taxon (Willumsen, 2010).

Cerebrocysta waipawaensis Wilson, 1988

Cerodinium medalfii (Stover 1974) Lentin & Williams 1987

Cerodinium striatum (Drugg, 1967) Lentin & Williams 1987

Cerodinium spp.

^{rw} *Cribroperidinium* sp.

^{rw} *Diconodinium cristatum* (Cookson & Eisenack 1974) Morgan 1977

Eisenackia circumtabulata Drugg, 1967

Eisenackia margarita (Harland 1979) Quattrocchio & Sarjeant 2003

Eisenackia reticulata (Damassa 1979) Quattrocchio & Sarjeant 2003 group

Remarks: This group includes the reticulate gonyaulacoid cysts *Eisenackia reticulata* (low penitabular processes) and the similar taxon *Cassidium fragile* (Harris 1965) Drugg, 1967 (no penitabular or intratabular processes). Both have a relatively thick-walled autophragm and low, coarse, reticulate intratabular sculpture. Grouping these specimens allows for comparison with the biostratigraphical ranges of Crouch et al. (2014), although data for the individual species is kept separate in Supplementary Table 1. Further, we recognise now that

specimens of *Eisenackia reticulata* that were previously thought to be reworked above the K–Pg boundary in D5.251 are probably *in situ* (Bowman et al., 2012).

Elytrocysta sp. of Askin (1988a)

Exochosphaeridium bifidum (Clarke & Verdier 1967) Clarke et al., 1968

Exochosphaeridium sp.

Hystrichosphaeridium tubiferum (Ehrenberg 1838) Deflandre 1937

Hystrichosphaeridium tubiferum (Ehrenberg 1838) Deflandre 1937

subsp. *brevispinum* (Davey & Williams 1966) Lentin & Williams 1973

Impagidinium cristatum (May 1980) Lentin & Williams 1981

Impagidinium maculatum (Cookson & Eisenack 1961) Stover & Evitt 1978

Impletosphaeridium clavus (Wrenn and Hart, 1988) Bowman et al., 2013b

Lejeunecysta hyalina (Gerlack 1961) Kjellström 1972.

Lingulodinium bergmannii (Archangelsky 1969) Quattrocchio & Sarjeant 2003

Manumiella conorata (Stover 1974) Bujak & Davies 1983

Manumiella druggii (Stover 1974) Bujak & Davies 1983

Remarks: Thorn et al. (2009) first noted the occurrence of a mesophragm in specimens of *Manumiella bertodano* Thorn et al., 2009, *Manumiella conorata* (Stover 1974) Bujak & Davies 1983 and *Manumiella seelandica* (Lange 1969) Bujak & Davies 1983 from Seymour Island. The presence of a mesophragm has now also been observed in specimens of *Manumiella druggii* in the current study (Fig. 3). [Note: *Manumiella bertodano* Thorn et al., 2009 is now considered to be conspecific with *Alterbidinium longicornutum* Roncaglia et al. 1999. This necessitates a name change for the latest Cretaceous *Manumiella bertodano* Interval Zone in Bowman et al. (2012) to *Alterbidinium longicornutum* Interval Zone. The zone characteristics remain the same.]

Manumiella seelandica (Lange 1969) Bujak & Davies 1983

Manumiella rotunda Wilson, 1988

Remarks: These rare specimens have a rounded to slightly ovoid outline and are circumcavate, with an apical pericoel that varies in development. There is either no apical protuberance, or a slight nipple-like protrusion, and no antapical horns (Fig. 3). Reticulum development varies. Crouch et al. (2014) note morphological variation within their specimens compared with the type specimens of Wilson (1988), but consider this to be within the definition of the species. We agree, and our specimens from Seymour Island compare well to those illustrated and described by Crouch et al. (2014). *Manumiella rotunda* is only known from the Paleocene of the mid to high southern latitudes (e.g. Röhl et al., 2004; Hollis et al., 2014) with this record from uppermost D9.605 being the first from the Antarctic.

Microdinium sp. 1

Remarks: Spheroidal to ovoidal in outline. Low, sutural ridges. Smooth surface. Apical archeopyle. Width: 25 (27) 30 µm; Height: 28 (30) 33 µm (n = 7).

Microdinium? sp.

Remarks: Similar to *Microdinium* sp.1, but slightly larger and less robust. Granular to finely reticulate surface. Questionably assigned to this genus. Width: 33 (35) 38 µm; Height: 33 (38) 40 µm (n = 6).

^{rw} *Odontochitina porifera* Cookson 1956

^{rw} *Odontochitina spinosa* Wilson, 1984

Operculodinium sp. 1

Remarks: Subspherical to ovoidal in outline. Surface smooth to finely granular. Numerous non-tabular processes, distally solid and capitate. Precingular archeopyle. Processes up to ~10 µm long; Cyst body width: 24 (31) 37 µm; length: 28 (35) 41 µm (n = 4).

Operculodinium spp.

Palaeocystodinium australinum (Cookson 1965) Lentin & Williams 1976

Palaeocystodinium golzowense Alberti 1961

Remarks: Specimens include those that compare closely with the original description (long, tapering horns, delicate membranes), but

also some with a dark-coloured inner body and slight thickening in the horns.

Palaeocystodinium granulatum (Wilson 1967) Lentin & Williams 1976

Palaeocystodinium lidiae (Górka 1963) Davey 1969

Palaeocystodinium spp.

Remarks: As noted by Wrenn and Hart (1988) as *Palaeocystodinium* sp. indet., isolated epicysts of *Palaeocystodinium australinum* and *Palaeocystodinium golzowense* are indistinguishable – we prefer to include them here as *Palaeocystodinium* spp. Isolated hypocysts from these species can be distinguished by the presence (*Palaeocystodinium australinum*) or absence (*Palaeocystodinium golzowense*) of accessory antapical horns.

Palaeoperidinium pyrophorum (Ehrenberg 1838 ex Wetzel 1933) Sarjeant 1967 emend. Evitt et al. 1998

Remarks: The HCO of *Palaeoperidinium pyrophorum* (at 324.3 m in D9.605 on Seymour Island) is heterochronous across this region. At ODP Site 1172 on the East Tasman Plateau, this bioevent (defining the base of zone SPDZ1) is correlated to the base of Subchron C26n, close to the Selandian–Thanetian boundary at -59.2 ± 0.2 Ma (Bijl et al., 2013). In the New Zealand east coast basins, the HCO occurs much earlier (~ 4.3 myrs) within lowermost C27r (~ 63.5 Ma, mid Danian; Crouch et al., 2014, fig. 14), immediately below the NZDP3/NZDP4 boundary. We consider the worldwide heterochroneity of this bioevent, as noted by Crouch et al. (2014, p. 77) to be effectively floating in time. It is therefore likely to be dependent on regional palaeoenvironmental factors rather than any global event and is not used specifically here for biostratigraphical correlation.

The HO of *Palaeoperidinium pyrophorum*, despite being a heterochronous event worldwide (Crouch et al., 2014), is apparently isochronous within the southern mid to high palaeolatitudes. It occurs within the uppermost part of NZDP4 in New Zealand, the upper boundary of which is dated at ~ 62.5 Ma (Crouch et al., 2014). This is consistent with the top of the *Palaeoperidinium pyrophorum* Zone of the Gippsland Basin, Australia, also dated at 62.5 Ma (Partridge, 2006). All dates quoted herein from Partridge (2006) are updated to the timescale of Gradstein et al. (2012). The known range of the HO of this taxon is from the late Danian to latest Selandian (Crouch et al., 2014).

Phelodinium cf. *magnificum* (Stanley 1965) Stover & Evitt 1978

Remarks: As noted in Bowman et al. (2012), specimens of this taxon observed in the Seymour Island sequence are smaller than the type material.

Senegalinium obscurum (Drugg, 1967) Stover & Evitt 1978

Senegalinium? *dilwynense* (Cookson & Eisenack 1965) Stover & Evitt 1978

Spinidinium colemanii Wrenn and Hart, 1988

Remarks: These densely spinulose cysts we consider fit within the species description of *Spinidinium colemanii*. This taxa was listed as *Spinidinium* sp. 1 of Askin (1988a) in section D5.251 (Bowman et al., 2012).

Spinidinium densispinatum (Stanley 1965) Sluijs et al., 2009

Spinidinium essoii (Cookson & Eisenack 1967) Sluijs et al., 2009

Spinidinium cf. *lanterna* (Cookson & Eisenack 1970) Sluijs et al., 2009

Remarks: Specimens assigned to *Spinidinium* cf. *lanterna* show a morphological continuum between two end members. The first is similar to the original description for the species with a distinctly rhomboidal outline, an endocyst that almost completely fills the pericoel and dense, needle-like spines. The second is more “lantern-like” in outline with a more globular endocyst that does not fill the pericoel and with less dense, coarser spines. This second end member was illustrated by Askin (1988a) as *Spinidinium* cf. *lanterna* and by Wrenn and Hart (1988) as *Spinidinium lanterna*.

Spinidinium sp. A [“A” to differentiate it easily from *Spinidinium* sp. 1 of Askin, 1988a]

Remarks: This spinidinioid peridinialean dinoflagellate cyst has a stenodeltaform archeopyle, which is often difficult to discern, as the 4th

plate remains attached. It has sutural crests and very few spines. We use the revised diagnosis of *Spinidinium* (Cookson & Eisenack 1962) Sluijs et al., 2009.

Spinidinium spp.

Spiniferites ramosus (Ehrenberg 1838) Mantell 1854

Spiniferites ramosus (Ehrenberg 1838) Mantell 1854 subsp. *reticulatus* (Davey & Williams 1966) Lentin & Williams 1973

Spiniferites sp.

Tanyosphaeridium xanthiopyxides (Wetzel 1933 ex Deflandre 1937) Stover & Evitt 1978

Tectatodinium sp. 1

Remarks: This round, thick-walled cyst resembles *Tectatodinium pellitum* Wall (1967) Head, 1994 with a thick, spongy luxuria. However, *Tectatodinium pellitum* has a distinctive irregular margin to the archeopyle, whereas the opercula of the cysts observed herein are consistently smooth and rounded. *Habibacysta tectata* Head et al. 1989 also has similar gross morphology, with rounded edges and smooth margins to the operculum, but is distinguished from the cysts observed herein by its thinner wall and presence of columnellae (Head, 1994). The thick spongy luxuria places the observed cysts in the genus *Tectatodinium* (Wall 1967) Head, 1994, which has only two species (*Tectatodinium pellitum* and *Tectatodinium rugulatum* (Hansen, 1977) McMinn, 1988; Fensome and Williams, 2004), which may be conspecific (Head, 1994). It is likely that the cysts observed herein are a new species.

Trithyrodinium evittii Drugg, 1967

Vozzhennikovia angulata (Wilson, 1988) Sluijs et al., 2009

Remarks: Specimens assigned here to *Vozzhennikovia angulata* are distinguished from *Spinidinium densispinatum* by a distinctly angular outline and more robust cyst walls.

Xenicodinium cf. *reticulatum* Hansen, 1977

Remarks: Chorate. Closely appressed endophragm and periphragm between processes. Precingular archeopyle, but otherwise no indication of paratabulation. Process bases connected by septa that give the cyst a reticulate to meandriform appearance.

Xenicodinium sp. 1

Remarks: This rare, but distinctive cyst has a thin ($\sim 1 \mu\text{m}$ thick) autophragm, characteristically muddy brown in colour. Subspherical to ovoidal in outline. Densely covered with short, fine, non-tabular processes. Archeopyle type is uncertain, but on some specimens appears precingular. Width: 30, 32, 35; Height: 34, 36, 36 (n = 3).

Indeterminate dinoflagellate cysts

Appendix B. Additional fossil taxa discussed herein

Apectodinium hyperacanthum (Cookson & Eisenack 1965) Lentin & Williams 1977

Austrosphaera spp.

Carpatella cornuta (Grigorovich 1969) Damassa 1988

Damassadinium californicum (Drugg, 1967) Fensome et al. 1993

Hemiaulus incurvus Schibkova in Krotov and Schibkova, 1959

Heteroterma spp.

Naviculopsis spp.

Palamblages spp.

Pseudotylostoma spp.

Senoniasphaera inornata (Drugg 1970) Stover & Evitt 1978

Taioma spp.

‘*Thyasira*’ *townsendi* White 1887

Remarks: The genus name is placed in quotation marks due to this uncertain taxonomic assignment, after Little et al. (2015) and references therein.

References

Açikalin, S., Vellekoop, J., Ocakoğlu, F., Yılmaz, I.Ö., Smit, J., Altner, S.Ö., Goderis, S., Vonhof, H., Speijer, R.P., Woelders, L., Fornaciari, E., Brinkhuis, H., 2015. Geochemical and palaeontological characterization of a new K–Pg boundary locality from the northern

- branch of the Neo-Tethys: Mudurnu – Göynük Basin, NW Turkey. *Cretaceous Research* 52, 251–267.
- Askin, R.A., 1988a. Campanian to Paleocene palynological succession of Seymour and adjacent islands, northeastern Antarctic Peninsula. In: Feldmann, R.M., Woodburne, M.O. (Eds.), *Geology and Paleontology of Seymour Island*. Geological Society of America Memoir 169, pp. 131–153.
- Askin, R.A., 1988b. The palynological record across the Cretaceous/Tertiary transition on Seymour Island, Antarctica. In: Feldmann, R.M., Woodburne, M.O. (Eds.), *Geology and Paleontology of Seymour Island*. Geological Society of America Memoir 169, pp. 155–162.
- Askin, R.A., Jacobson, S.R., 1996. Palynological change across the Cretaceous–Tertiary boundary on Seymour Island, Antarctica: environmental and depositional factors. In: Macleod, N., Keller, G. (Eds.), *The Cretaceous–Tertiary Mass Extinction: Biotic and Environmental Events*. W.W. Norton & Co., New York, pp. 7–25.
- Bache, F., Mortimer, N., Sutherland, R., Collot, J., Rouillard, P., Stagpoole, V., Nicol, A., 2014. Seismic stratigraphic record of transition from Mesozoic subduction to continental breakup in the Zealandia sector of eastern Gondwana. *Gondwana Research* 26, 1060–1078.
- Barker, P.E., Kennett, J.P., et al., 1988. Proceedings of the Ocean Drilling Program, Initial Reports. p. 113. <http://dx.doi.org/10.2973/odp.proc.ir.113.1988>.
- Beu, A.G., Maxwell, P.A., 1990. Cenozoic mollusca of New Zealand. *New Zealand Geological Survey Paleontological Bulletin* 58 (518 pp.).
- Beu, A.G., Raine, J.L., 2009. Revised Descriptions of New Zealand Cenozoic Mollusca from Beu and Maxwell (1990). *GNS Science Miscellaneous Series* 27.
- Bialas, R.W., Buck, W.R., Studinger, M., Fitzgerald, P., 2007. Plateau collapse model for the Transantarctic Mountains–West Antarctic rift system: insights from numerical experiments. *Geology* 35, 687–690.
- Bijl, P.K., Pross, J., Warnaar, J., Stickley, C.E., Huber, M., Guerstein, R., Houben, A.J.P., Sluijs, A., Visscher, H., Brinkhuis, H., 2011. Environmental forcings of Paleogene Southern Ocean dinoflagellate biogeography. *Paleoceanography* 26, PA 1202. <http://dx.doi.org/10.1029/2009PA001905>.
- Bijl, P.K., Sluijs, A., Brinkhuis, H., 2013. A magneto- and chemostratigraphically calibrated dinoflagellate cyst zonation of the early Paleogene South Pacific Ocean. *Earth-Science Reviews* 124, 1–31.
- Boger, S.D., 2011. Antarctica – before and after Gondwana. *Gondwana Research* 19, 335–371.
- Bowman, V.C., Francis, J.E., Riding, J.B., Hunter, S.J., Haywood, A.M., 2012. A latest Cretaceous to earliest Paleogene dinoflagellate cyst zonation from Antarctica, and implications for phytoprovincialism in the high southern latitudes. *Review of Palaeobotany and Palynology* 171, 40–56.
- Bowman, V.C., Francis, J.E., Riding, J.B., 2013a. Late Cretaceous winter sea ice in Antarctica? *Geology* 41, 1227–1230.
- Bowman, V.C., Francis, J.E., Riding, J.B., Crame, J.A., Hannah, M.J., 2013b. The taxonomy and palaeobiogeography of small chorate dinoflagellate cysts from the Late Cretaceous to Quaternary of Antarctica. *Palynology* 37, 151–169.
- Bowman, V.C., Francis, J.E., Askin, R.A., Riding, J.B., Swindles, G.T., 2014. Latest Cretaceous–earliest Paleogene vegetation and climate change at the high southern latitudes: palynological evidence from Seymour Island, Antarctic Peninsula. *Palaeogeography, Palaeoclimatology, Palaeoecology* 408, 26–47.
- Cande, S.C., Stock, J.M., 2004. Cenozoic reconstructions of the Australia–New Zealand–South Pacific sector of Antarctica. In: Exon, N., Kennett, J.P., Malone, M. (Eds.), *The Cenozoic Southern Ocean*. AGU Geophysical Monograph, Washington DC, USA, pp. 5–18.
- Cantrill, D.J., Poole, I., 2002. Cretaceous patterns of floristic change in the Antarctic Peninsula. In: Crame, J.A., Owen, A.W. (Eds.), *Palaeobiogeography and Biodiversity Change: The Ordovician and Mesozoic–Cenozoic Radiations*. Geological Society, London, Special Publications 194, pp. 141–152.
- Case, J.A., 1988. Paleogene floras from Seymour Island, Antarctic Peninsula. In: Feldmann, R.M., Woodburne, M.O. (Eds.), *Geology and Paleontology of Seymour Island*. Geological Society of America Memoir 169, pp. 523–530.
- Chenet, A.-L., Courtillot, V., Fluteau, F., Gérard, M., Quidelleur, X., Khadri, S.F.R., Subbarao, K.V., Thordarson, T., 2009. Determination of rapid Deccan eruptions across the Cretaceous–Tertiary boundary using paleomagnetic secular variation: 2. Constraints from analysis of eight new sections and synthesis for a 3500-m-thick composite section. *Journal of Geophysical Research* 114, B06103. <http://dx.doi.org/10.1029/2008JB005644>.
- Condon, D.J., Schoene, R.B., McLean, N.M., Parrish, R., Bowring, S.A., 2015. Metrology and traceability of U–Pb isotope dilution geochronology (EARTHTIME tracer calibration Part I). *Geochimica et Cosmochimica Acta*. <http://dx.doi.org/10.1016/j.gca.2015.05.026>.
- Courtillot, V., Fluteau, F., 2010. Cretaceous extinctions: the volcanic hypothesis. *Science* 328, 973–974.
- Crame, J.A., 2013. Early Cenozoic differentiation of polar marine faunas. *PLoS One* 8, e54139. <http://dx.doi.org/10.1371/journal.pone.0054139>.
- Crame, J.A., Francis, J.E., Cantrill, D.J., Pirrie, D., 2004. Maastrichtian stratigraphy of Antarctica. *Cretaceous Research* 25, 411–423.
- Crame, J.A., Beu, A.G., Ineson, J.R., Francis, J.E., Whittle, R.J., Bowman, V.C., 2014. The early origin of the Antarctic marine fauna and its evolutionary implications. *PLoS One* 9, e114743. <http://dx.doi.org/10.1371/journal.pone.0114743>.
- Crouch, E.M., Heilmann-Clausen, C., Brinkhuis, H., Morgans, H.E.G., Rogers, K.M., Egger, H., Schmitz, B., 2001. Global dinoflagellate event associated with the late Paleocene thermal maximum. *Geology* 29, 315–318.
- Crouch, E.M., Brinkhuis, H., Visscher, H., Adatte, T., Bolle, M.-P., 2003a. Late Paleocene–early Eocene dinoflagellate cyst records from the Tethys: further observations on the global distribution of *Apectodinium*. In: Wing, S.L., Gingerich, P.D., Schmitz, B., Thomas, E. (Eds.), *Causes and Consequences of Globally Warm Climates in the Early Paleogene*. Geological Society of America Special Paper 369, pp. 113–131.
- Crouch, E.M., Dickens, G.R., Brinkhuis, H., Aubrey, M.-P., Hollis, C.J., Rogers, K.M., Visscher, H., 2003b. The *Apectodinium* acme and terrestrial discharge during the Paleocene–Eocene thermal maximum: new palynological, geochemical and calcareous nannoplankton observations at Tawanui, New Zealand. *Palaeogeography, Palaeoclimatology, Palaeoecology* 194, 387–403.
- Crouch, E.M., Willumsen, P.S., Kulhanek, D.K., Gibbs, S., 2014. A revised Paleocene (Teurian) dinoflagellate cyst zonation from eastern New Zealand. *Review of Palaeobotany and Palynology* 202, 47–79.
- Dalziel, I.W.D., Lawver, L.A., 2001. The lithospheric setting of the West Antarctic Ice Sheet. In: Alley, R.B., Bindschadler, R.A. (Eds.), *The West Antarctic Ice Sheet: Behavior and Environment*. American Geophysical Union Antarctic Research Series 77, pp. 29–44.
- Dam, G., Nøhr-Hansen, H., Kennedy, W.J., 1998. The northernmost marine Cretaceous–Tertiary boundary section: Nuussuaq, West Greenland. *Geology of Greenland Survey Bulletin* 180, 138–144.
- Davey, F.J., Brancolini, G., 1987. The late Mesozoic and Cenozoic structural setting of the Ross Sea region. In: Cooper, A.K., Barker, P.F., Brancolini, G. (Eds.), *Geology and Seismic Stratigraphy of the Antarctic Margin*. American Geophysical Union Antarctic Research Series 68, pp. 167–182.
- Decesari, R.C., Wilson, D.S., Luyendyk, B.P., Faulkner, M., 2007. Cretaceous and Tertiary extension throughout the Ross Sea, Antarctica. In: Cooper, A.K., Barrett, P.J., Stagg, H., Storey, B., Stump, E., Wise, W., the 10th ISAES editorial team, W. (Eds.), *Antarctica: A Keystone in a Changing World*. Proceedings of the 10th International Symposium on Antarctic Earth Sciences Short Research Paper 098. The National Academies Press, Washington, D.C., p. 4. <http://dx.doi.org/10.3133/of2007-1047.srp098>.
- del Rio, C.J., 2012. A new Early Danian gastropod assemblage from northern Patagonia (Río Negro Province, Argentina). *Journal of Paleontology* 86, 1002–1016.
- Drugg, W.S., 1967. Palynology of the upper Moreno Formation (Late Cretaceous–Paleocene) Escarpado Canyon, California. *Palaeontographica Abteilung B* 120, 1–71.
- Eagles, G., Jokat, W., 2014. Tectonic reconstructions for paleobathymetry in Drake Passage. *Tectonophysics* 611, 28–50.
- Elliot, D.H., 2013. The geological and tectonic evolution of the Transantarctic Mountains: a review. In: Hambrey, M.J., Barker, P.F., Barrett, P.J., Bowman, V., Davies, B., Smellie, J.L., Tranter, M. (Eds.), *Antarctic Palaeoenvironments and Earth-Surface Processes*. Geological Society, London, Special Publications 381, pp. 7–35.
- Elliot, D.H., Askin, R.A., Kyte, F.T., Zinsmeister, W.J., 1994. Iridium and dinocysts at the Cretaceous–Tertiary boundary on Seymour Island, Antarctica: implications for the K–T event. *Geology* 22, 675–678.
- Fensome, R.A., Williams, G.L., 2004. The Lentini and Williams index of fossil dinoflagellates 2004 edition. *AASP Contributions Series* 42. American Association of Stratigraphic Palynologists Foundation (909 pp.).
- Fensome, R.A., Williams, G.L., MacRae, R.A., 2009. Late Cretaceous and Cenozoic fossil dinoflagellates and other palynomorphs from the Scotian Margin, offshore eastern Canada. *Journal of Systematic Palaeontology* 7, 1–79.
- Ferraccioli, F., Finn, C.A., Jordan, T.A., Bell, R.E., Anderson, L.M., Damaske, D., 2011. East Antarctic rifting triggers uplift of the Gamburtsev Mountains. *Nature* 479, 388–392.
- Finlay, H.J., Marwick, J., 1937. The Wangaloan and associated molluscan faunas of Kaitangata–Green Island subdivision. Part 1 – the Wangaloan fauna. *New Zealand Geological Survey Paleontological Bulletin* 15 (140 pp.).
- Fitzgerald, P.G., Stump, E., 1991. Early Cretaceous uplift in the Ellsworth Mountains of West Antarctica. *Science* 254, 92–94.
- Fretwell, P., Pritchard, H.D., et al., 2013. Bedmap2: improved ice bed, surface and thickness datasets for Antarctica. *The Cryosphere* 7, 375–393.
- Gaina, C., Muller, R.D., Royer, J.Y., Stock, J.M., Hardebeck, J., Symonds, P., 1998. The tectonic history of the Tasman Sea: a puzzle with thirteen pieces. *Journal of Geophysical Research* 103, 12413–12433.
- Gao, Y., Ibarra, D.E., Wang, C., Caves, J.K., Chamberlain, C.P., Graham, S.A., Wu, H., 2015. Mid-latitude terrestrial climate of East Asia linked to global climate in the Late Cretaceous. *Geology*. <http://dx.doi.org/10.1130/G36427.1>.
- Gradstein, F.M., Ogg, J.G., Schmitz, M.D., Ogg, G.M., 2012. *The Geological Time Scale 2012*. Elsevier (1176 pp.).
- Griffin, M., Hunicken, M.A., 1994. Late Cretaceous–Early Tertiary gastropods from southwestern Patagonia, Argentina. *Journal of Paleontology* 68, 257–274.
- Grunow, A.M., Kent, D.V., Dalziel, I.W.D., 1991. New paleomagnetic data from Thurston Island: implications for the tectonics of West Antarctica and Weddell Sea opening. *Journal of Geophysical Research* 96 (B11), 17935–17954.
- Hansen, J.M., 1977. Dinoflagellate stratigraphy and echinoid distribution in Upper Maastrichtian and Danian deposits from Denmark. *Bulletin of the Geological Society of Denmark* 26, 1–26.
- Harwood, D.M., 1988. Upper Cretaceous and lower Paleocene diatom and silicoflagellate biostratigraphy of Seymour Island, eastern Antarctic Peninsula. In: Feldmann, R.M., Woodburne, M.O. (Eds.), *Geology and Paleontology of Seymour Island*. Geological Society of America Memoir 169, pp. 55–129.
- Hathway, B., 2000. Continental rift to back-arc basin: Jurassic–Cretaceous stratigraphical and structural evolution of the Larsen Basin, Antarctic Peninsula. *Journal of the Geological Society of London* 157, 417–432.
- Head, M.J., 1994. Morphology and palaeoenvironmental significance of the Cenozoic dinoflagellate genera *Tectatodinium* and *Habibacysta*. *Micropaleontology* 40, 289–321.
- Heilmann-Clausen, C., 1985. Dinoflagellate stratigraphy of the uppermost Danian to Ypresian in the Viborg 1 borehole, central Jylland, Denmark. *Danmarks Geologiske Undersøgelse, Serie A* 7 (69 pp.).
- Helby, R., Morgan, R., Partridge, A.D., 1987. A palynological zonation of the Australian Mesozoic. *Association of Australasian Palaeontologists Memoir* 4, 1–94.
- Henderson, R.A., 1970. Ammonoidea from the Mata Series (Santonian–Maastrichtian) of New Zealand. *Special Papers in Palaeontology* 6, 1–82.
- Hollis, C., 2003. The Cretaceous/Tertiary boundary event in New Zealand: profiling mass extinction. *New Zealand Journal of Geology and Geophysics* 46, 307–321.

- Hollis, C.J., Taylor, K.W.R., Handley, L., Pancost, R.D., Huber, M., Creech, J.B., Hines, B.R., Crouch, E.M., Morgans, H.E.G., Crampton, J.S., Gibbs, S., Pearson, P.N., Zachos, J.C., 2012. Early Paleogene temperature history of the southwest Pacific Ocean: reconciling proxies and models. *Earth and Planetary Science Letters* 349–350, 53–66.
- Hollis, C.J., Taylor, M.J.S., Andrew, B., Taylor, K.W., Lurcock, P., Bijl, P.K., Kulhanek, D.K., Crouch, E.M., Nelson, C.S., Pancost, R.D., Huber, M., Wilson, G.S., Ventura, T., Crampton, J.S., Schiøler, P., Phillips, A., 2014. Organic-rich sedimentation in the South Pacific Ocean associated with Late Paleocene climatic cooling. *Earth-Science Reviews* 134, 81–97.
- Huber, B.T., 1988. Upper Campanian–Paleocene foraminifera from the James Ross Island region, Antarctic Peninsula. In: Feldmann, R.M., Woodburne, M.O. (Eds.), *Geology and Paleontology of Seymour Island*. Geological Society of America Memoir 169, pp. 163–252.
- Huber, M., Brinhius, H., Stickley, C.E., Döös, K., Sluijs, A., Warnaar, J., Schellenberg, S.A., Williams, G.L., 2004. Eocene circulation of the Southern Ocean: was Antarctica kept warm by subtropical waters? *Paleoceanography* 19, PA 4026. <http://dx.doi.org/10.1029/2004PA001014>.
- Huerta, A.S., Harry, D.L., 2007. The transition from diffuse to focused extension: modeled evolution of the West Antarctic rift system. *Earth and Planetary Science Letters* 255, 133–147.
- Hultberg, S.U., 1986. Danian dinoflagellate zonation, the C–T boundary and the stratigraphical position of the fish clay in southern Scandinavia. *Journal of Micropaleontology* 5, 37–47.
- Hunter, S.J., 2009. Modelling Antarctic ice sheets under greenhouse earth conditions. Unpublished Ph.D. thesis. University of Leeds, 321 pp.
- Jordan, T.A., Ferraccioli, F., Armadillo, E., Bozzo, E., 2013. Crustal architecture of the Wilkes subglacial basin in East Antarctica, as revealed from airborne gravity data. *Tectonophysics* 585, 196–206.
- Katz, M.E., Cramer, B.S., Toggweiler, J.R., Esmay, G., Liu, C., Miller, K.G., Rosenthal, Y., Wade, B.S., Wright, J.D., 2011. Impact of Antarctic circumpolar current development on late Paleogene ocean structure. *Science* 332, 1076–1079.
- King, P.R., Naish, T.R., Browne, G.H., Field, B.D., Edbrooke, S.W., 1999. Cretaceous to Recent Sedimentary Patterns in New Zealand. Institute of Geological and Antarctic Sciences folio series 1.
- Krotov, A.I., Schibkova, K.G., 1959. Species novae diatomacearum e Paleogeno montium uralensium. Neue diatomeen arten aus dem Paläogen des Urals (New species of diatoms from the Paleogene sediments of the Urals). *Botanicheskie Materialy, Otdela Sporovykh Rastenii, Botanicheskii Institut, Akademiya Nauk U.S.S.R.* 12, 112–129.
- Laird, M.G., Bradshaw, J.D., 2004. The break-up of a long-term relationship: the Cretaceous separation of New Zealand from Gondwana. *Gondwana Research* 7, 273–286.
- Larter, R.D., Cunningham, A.P., Barker, P.F., Gohl, K., Nitsche, F.O., 2002. Tectonic evolution of the Pacific margin of Antarctica – 1 Late Cretaceous tectonic reconstructions. *Journal of Geophysical Research* 107 (B12), 2345. <http://dx.doi.org/10.1029/2000JB000052>.
- Lawver, L.A., Gahagan, L.M., Coffin, M.F., 1992. The Development of Paleoseaways Around Antarctica. In: Kennett, J.P., Warnke, D.A. (Eds.), *The Antarctic Paleoenvironment: A Perspective on Global Change, Part 1*. American Geophysical Union Antarctic Research Series 56, pp. 7–30.
- Levy, R.H., Harwood, D.M., 2000. Tertiary marine palynomorphs from the McMurdo Sound Erratics, Antarctica. In: Stilwell, J.D., Feldmann, M. (Eds.), *Paleobiology and Paleoenvironments of Eocene Rocks, McMurdo Sound, East Antarctica*. American Geophysical Union Antarctic Research Series 76, pp. 183–242.
- Lisker, F., Läufer, A.L., 2013. The Mesozoic Victoria Basin: vanished link between Antarctica and Australia. *Geology* 41, 1043–1046.
- Little, C.T.S., Birgel, D., Boyce, A.J., Crame, J.A., Francis, J.E., Kiel, S., Peckmann, J., Pirrie, D., Rollinson, G.K., Witts, J.D., 2015. Late Cretaceous (Maastrichtian) shallow water hydrocarbon seeps from Snow Hill and Seymour Islands, James Ross Basin, Antarctica. *Paleogeography, Palaeoclimatology, Palaeoecology* 418, 213–228.
- Macellari, C.E., 1984. Late Cretaceous stratigraphy, sedimentology and micropaleontology of Seymour Island, Antarctic Peninsula. Unpublished Ph.D. thesis, Ohio State University, 599 pp.
- Macellari, C.E., 1988. Stratigraphy, sedimentology, and paleoecology of Upper Cretaceous/Paleocene shelf-deltaic sediments of Seymour Island. In: Feldmann, R.M., Woodburne, M.O. (Eds.), *Geology and Paleontology of Seymour Island*. Geological Society of America Memoir 169, pp. 25–53.
- Marenssi, S.A., Santillana, S.N., Bauer, M., 2012. Estratigrafía, petrografía sedimentaria y procedencia de las formaciones Sobral y Cross Valley (Paleoceno), Isla Marambio (Seymour), Antártida. *Andean Geology* 39, 67–91.
- Markwick, P.J., Valdes, P.J., 2004. Palaeo-digital elevation models for use as boundary conditions in coupled ocean–atmosphere GCM experiments: a Maastrichtian (Late Cretaceous) example. *Paleogeography, Palaeoclimatology, Palaeoecology* 213, 37–63.
- Martos, Y.M., Catalán, M., Galindo-Zaldívar, J., Maldonado, A., Bohoyo, F., 2014. Insights about the structure and evolution of the Scotia Arc from a new magnetic data compilation. *Global and Planetary Change* 123, 239–248.
- Mattinson, J.M., 2005. Zircon U–Pb chemical abrasion (“CA-TIMS”) method: combined annealing and multi-step partial dissolution analysis for improved precision and accuracy of zircon ages. *Chemical Geology* 220, 47–66.
- McArthur, J.M., Thirlwall, M.F., Engkilde, M., Zinsmeister, W.J., Howarth, R.J., 1998. Strontium isotope profiles across K/T boundary sequences in Denmark and Antarctica. *Earth and Planetary Science Letters* 160, 179–192.
- McArthur, J.M., Howarth, R.J., Shields, G.A., 2012. Strontium isotope stratigraphy. In: Gradstein, F.M., Ogg, J.G., Schmitz, M., Ogg, G. (Eds.), *The Geologic Time Scale 2012*. Elsevier, pp. 127–144.
- McLean, N.M., Condon, D.J., Blair Schoene, R., Bowring, S.A., 2015. Evaluating uncertainties in the calibration of isotopic reference materials and multi-element isotopic tracers (EARTHTIME Tracer Calibration Part II). *Geochimica et Cosmochimica Acta*. <http://dx.doi.org/10.1016/j.gca.2015.02.040>.
- McMinn, A., 1988. Outline of a Late Cretaceous dinoflagellate zonation of northwestern Australia. *Alcheringa* 12, 137–156.
- M’Hamdi, A., Slimani, H., Ismail-Latrache, K.B., Soussi, M., 2013. Biostratigraphie des kystes de dinoflagellés de la limite Crétacé–Paléogène à Ellès, Tunisie. *Revue de Micropaleontologie* 56, 27–42.
- Michaux, B., 2009. Reciprocity between biology and geology: reconstructing polar Gondwana. *Gondwana Research* 16, 655–668.
- Miller, K.G., Wright, J.D., Katz, M.E., Browning, J.V., Cramer, B.S., Wade, B.S., Mizintseva, S.F., 2008. A view of Antarctic ice-sheet evolution from sea-level changes and deep-sea isotopes changes during the Late Cretaceous–Cenozoic. In: Cooper, A.K., Barrett, P.J., Stagg, H., Storey, B., Stump, E., Wise, W., the 10th ISAES editorial team (Eds.), *Antarctica: A Keystone in a Changing World*. Proceedings of the 10th International Symposium on Antarctic Earth Sciences. The National Academies Press, Washington, D.C. <http://dx.doi.org/10.3133/of2007-1047.kp06>.
- Mohr, B.A.R., 1990. Eocene and Oligocene sporomorphs and dinoflagellate cysts from Leg 113 drill sites, Weddell Sea, Antarctica. In: Barker, P.F., Kennett, J.P., et al. (Eds.), *Proceedings of the Ocean Drilling Program Scientific Results* 113, pp. 595–612.
- Molina, E., 2015. Evidence and causes of the main extinction events in the Paleogene based on extinction and survival patterns of foraminifera. *Earth-Science Reviews* 140, 166–181.
- Montes, M., Nozal, F., Santillana, S., Marenssi, S.A., Olivero, E., 2010. Mapa geológico de la Isla Marambio (Seymour). Escala 1:20,000. Argentino y Instituto Geológico y Minero de España, Instituto Antártico.
- Mortimer, N., 2004. New Zealand’s geological foundations. *Gondwana Research* 7, 261–272.
- Mudge, D.C., Bujak, J.P., 2001. Biostratigraphic evidence for evolving palaeoenvironments in the Lower Paleogene of the Faeroe–Shetland Basin. *Marine and Petroleum Geology* 18, 577–590.
- Mukasa, S.B., Dalziel, I.W.D., 2000. Marie Byrd Land, West Antarctica: evolution of Gondwana’s Pacific margin constrained by zircon U–Pb geochronology and feldspar common-Pb isotopic compositions. *GSA Bulletin* 112, 611–627.
- Nøhr-Hansen, H., Dam, G., 1999. *Trithyrodinium evittii* Drugg 1967 and *T. fragile* Davey 1969 an artificially split of one dinoflagellate cyst species – stratigraphic and palaeoenvironmental importance. *Grana* 38, 125–133.
- Olivero, E.B., 2012. Sedimentary cycles, ammonite diversity and palaeoenvironmental changes in the Upper Cretaceous Marambio Group, Antarctica. *Cretaceous Research* 34, 348–366.
- Olivero, E.B., Medina, F.A., 2000. Patterns of Late Cretaceous ammonite biogeography in southern high latitudes: the family Kossmaticeratidae in Antarctica. *Cretaceous Research* 21, 269–279.
- Olivero, E.B., Zinsmeister, W.J., 1989. Large heteromorph ammonites from the Upper Cretaceous of Seymour Island, Antarctica. *Journal of Paleontology* 63, 626–636.
- Olivero, E.B., Ponce, J.J., Marsicano, C.A., Martinioni, D.R., 2007. Depositional settings of the basal López de Bertodano Formation, Maastrichtian, Antarctica. *Revista de la Asociación Geológica Argentina* 62, 521–529.
- Olivero, E.B., Ponce, J.J., Martinioni, D.R., 2008. Sedimentology and architecture of sharp-based tidal sandstones in the upper Marambio Group, Maastrichtian of Antarctica. *Sedimentary Geology* 210, 11–26.
- Partridge, A.D., 2006. Late Cretaceous–Cenozoic palynology zonations, Gippsland Basin. In: Monteil, E. (Coordinator), *Australian Mesozoic and Cenozoic palynology Zonations – updated to the 2004 Geologic Time Scale*. Geoscience Australia Record 2006/23, Chart 4 of 4.
- Pedersen, G.K., Nøhr-Hansen, H., 2014. Sedimentary successions and palynofossil stratigraphy from the non-marine Lower Cretaceous to the marine Upper Cretaceous of the Nuussuaq Basin, West Greenland. *Bulletin of Canadian Petroleum Geology* 62, 261–288.
- Pirrie, D., Duane, A.M., Riding, J.B., 1992. Jurassic–Tertiary stratigraphy and palynology of the James Ross Basin: a review and introduction. *Antarctic Science* 4, 259–266.
- Powell, A.J., 1992. Dinoflagellate cysts of the Tertiary system. In: Powell, A.J. (Ed.), *A Stratigraphic Index of Dinoflagellate Cysts*. British Micropaleontological Society Publications Series. Chapman and Hall, London, pp. 155–251.
- Reguero, M., Goin, F., Hospitaleche, C.A., Dutra, T., Marenssi, S., 2013. Late Cretaceous/Paleogene West Antarctica Terrestrial Biota and its Intercontinental Affinities. Springer (120 pp.).
- Reguero, M.A., Gelfo, J.N., López, G.M., Bond, M., Abello, A., Santillana, S.N., Marenssi, S.A., 2014. Final Gondwana breakup: the Paleogene South American native ungulates and the demise of the South America–Antarctica land connection. *Global and Planetary Change* 123, 400–413.
- Röhl, U., Brinkhuis, H., Sluijs, A., Fuller, M., 2004. On the search for the Paleocene/Eocene boundary in the Southern Ocean: exploring ODP Leg 189 Holes 1171D and 1172D, Tasman Sea. In: Exon, N.F., Kennett, J.P., Malone, M.J. (Eds.), *The Cenozoic Southern Ocean: Tectonics, Sedimentation and Climate Change Between Australia and Antarctica*. Geophysical Monograph Series 151, pp. 113–125.
- Royer, D., 2006. CO₂-forced climate thresholds during the Phanerozoic. *Geochimica et Cosmochimica Acta* 70, 5665–5675.
- Sadler, P.M., 1988. Geometry and stratification of uppermost Cretaceous and Paleogene units on Seymour Island, Northern Antarctic Peninsula. In: Feldmann, R.M., Woodburne, M.O. (Eds.), *Geology and Paleontology of Seymour Island*. Geological Society of America Memoir 169, pp. 303–320.
- Salvini, F., Brancolini, G., Busetto, M., Storti, F., Mazzarini, F., Coren, F., 1997. Cenozoic geodynamics of the Ross Sea Region, Antarctica: crustal extension, intraplate strike-slip faulting and tectonic inheritance. *Journal of Geophysical Research* 102, 24669–24696.
- Santillana, S., Marenssi, S., 1997. Descripción e interpretación de las discordancias paleocenas de la isla Marambio, Antártica. *Jornadas Sobre Investigaciones Antárticas* 4, 262–266.
- Schoene, B., Samperton, K.M., Eddy, M.P., Keller, G., Adatte, T., Bowring, S.A., Khadri, S.F.R., Gertsch, B., 2014. U–Pb geochronology of the Deccan Traps and relation to the end-

- Cretaceous mass extinction. Science Express Reports. <http://dx.doi.org/10.1126/science.aaa0118>.
- Schulte, P., Alegret, L., Arenillas, I., et al., 2010. The Chicxulub asteroid impact and mass extinction at the Cretaceous–Paleogene boundary. *Science* 327, 1214–1218.
- Siddoway, C.S., 2008. Tectonics of the West Antarctic Rift System: new light on the history and dynamics of distributed intracontinental extension. In: Cooper, A.K., Barrett, P.J., Stagg, H., Storey, B., Stump, E., Wise, W., the 10th ISAES editorial team (Eds.), *Antarctica: A Keystone in a Changing World* Proceedings of the 10th International Symposium on Antarctic Earth Sciences Keynote Paper 09. The National Academies Press, Washington, D.C. <http://dx.doi.org/10.3133/of2007-1047.kp09>.
- Singer, B.S., Jicha, B.R., Condon, D.J., Macho, A.S., Hoffman, K.A., Dierkhising, J., Brown, M.C., Feinberg, J.M., Kidane, T., 2014. Precise ages of the Réunion event and Huckleberry Ridge excursion: episodic clustering of geomagnetic instabilities and the dynamics of flow within the outer core. *Earth and Planetary Science Letters* 405, 25–38.
- Sluijs, A., Brinkhuis, H., Williams, G.L., Fensome, R.A., 2009. Taxonomic revision of some Cretaceous–Cenozoic spiny organic-walled peridiniacean dinoflagellate cysts. *Review of Palaeobotany and Palynology* 154, 34–53.
- Stilwell, J.D., 2003. Patterns of biodiversity and faunal rebound following the K–T boundary extinction event in Austral Palaeocene molluscan faunas. *Palaeogeography, Palaeoclimatology, Palaeoecology* 195, 319–356.
- Stilwell, J.D., Zinsmeister, W.J., Oleinik, A.E., 2004. Early Paleocene molluscs of Antarctica: systematics, paleoecology and palaeobiogeographic significance. *Bulletins of American Paleontology* 367, 1–89.
- Storme, J.-Y., Steurbaut, E., Devleeschouwer, X., Dupuis, C., Iacumin, P., Rochez, G., Yans, J., 2014. Integrated bio-chemostratigraphical correlations and climatic evolution across the Danian–Selandian boundary at low latitudes. *Palaeogeography, Palaeoclimatology, Palaeoecology* 414, 212–224.
- Stover, L.E., Brinkhuis, H., Damassa, S.P., de Verteuil, L., Helby, R.J., Monteil, E., Partridge, A.D., Powell, A.J., Riding, J.B., Smelror, M., Williams, G.L., 1996. Mesozoic–Tertiary Dinoflagellates, Acritarchs and Prasinophytes. In: Jansonius, J., McGregor, D.C. (Eds.), *Palynology: Principles and Applications* vol. 2. American Association of Stratigraphic Palynologists Foundation, Dallas, pp. 641–750.
- Studinger, M., Bell, R.E., Buck, W.R., Karner, G.D., Blankenship, D.D., 2004. Sub-ice geology inland of the Transantarctic Mountains in light of new aerogeophysical data. *Earth and Planetary Science Letters* 220, 391–408.
- Sutherland, R., 1999. Basement geology and tectonic development of the greater New Zealand region: an interpretation from regional magnetic data. *Tectonophysics* 308, 341–362.
- Thomas, E., Barrera, E., Hamilton, N., Huber, B.T., Kennett, J.P., O'Connell, S.B., Pospichal, J.J., Speiß, V., Stott, L.D., Wei, W., Wise Jr., S.W., 1990. Upper Cretaceous–Paleogene Stratigraphy of Sites 689 and 690, Maud Rise (Antarctica). In: Barker, P.F., Kennett, J.P., et al. (Eds.), *Proceedings of the Ocean Drilling Program Scientific Results* 113, pp. 901–914.
- Thorn, V.C., Riding, J.B., Francis, J.E., 2009. The Late Cretaceous dinoflagellate cyst *Manumiella* – biostratigraphy, systematics, and paleoecological signals in Antarctica. *Review of Palaeobotany and Palynology* 156, 436–448.
- Tobin, T.S., Ward, P.D., Steig, E.J., Olivero, E.B., Hilburn, I.A., Mitchell, R.N., Diamond, M.R., Raub, T.D., Kirschvink, J.L., 2012. Extinction patterns, $\delta^{18}\text{O}$ trends, and magnetostratigraphy from a southern high-latitude Cretaceous–Paleogene section: links with Deccan volcanism. *Palaeogeography, Palaeoclimatology, Palaeoecology* 350–352, 180–188.
- Vandenbergh, N., Hilgen, F.J., Speijer, R.P., 2012. The Paleogene period. In: Gradstein, F.M., et al. (Eds.), *The Geologic Time Scale 2012*. Elsevier, pp. 855–921.
- Vaughan, A.P.M., Pankhurst, R.J., 2008. Tectonic overview of the West Gondwana margin. *Gondwana Research* 13, 150–162.
- Vellekoop, J., Smit, J., van der Schootbrugge, B., Weijers, J.W.H., Galeotti, S., Sinninghe Damsté, J.S., Brinkhuis, H., 2015. Palynological evidence for prolonged cooling along the Tunisian continental shelf following the K–Pg boundary impact. *Palaeogeography, Palaeoclimatology, Palaeoecology* 426, 216–228.
- Webb, P.N., 1979. Late Mesozoic–Cenozoic geology of the Ross sector, Antarctica. *Journal of the Royal Society of New Zealand* 11, 439–446.
- Webb, P.N., Neall, V.E., 1972. Cretaceous foraminifera in Quaternary deposits from Taylor Valley, Victoria Land. In: Adie, R.J. (Ed.), *Antarctic Geology and Geophysics*. Universitetsforlaget, Oslo, pp. 653–658.
- White, L.T., Gibson, G.M., Lister, G.S., 2013. A reassessment of palaeogeographic reconstructions of eastern Gondwana: bringing geology back into the equation. *Gondwana Research* 24, 984–998.
- Willumsen, P.S., 2004. Two new species of the dinoflagellate cyst genus *Carpatella* Grigorovich 1969 from the Cretaceous–Tertiary transition in New Zealand. *Journal of Micropalaeontology* 23, 119–125.
- Willumsen, P.S., 2010. Maastrichtian to Paleocene dinocysts from the Clarence Valley, South Island, New Zealand. *Alcheringa* 35, 199–240.
- Wilson, G.J., 1984. New Zealand Late Jurassic to Eocene dinoflagellate biostratigraphy – a summary. *Newsletters on Stratigraphy* 13, 104–117.
- Wilson, G.J., 1987. Dinoflagellate biostratigraphy of the Cretaceous–Tertiary boundary, mid-Waipara River section, North Canterbury, New Zealand. *New Zealand Geological Survey Record* 20, 8–15.
- Wilson, G.J., 1988. Paleocene and Eocene dinoflagellate cysts from Waipawa, Hawkes Bay, New Zealand. *New Zealand Geological Survey Paleontological Bulletin* 57 (96 pp.).
- Wilson, D.S., Luyendyk, B.P., 2009. West Antarctic palaeotopography estimated at the Eocene–Oligocene climate transition. *Geophysical Research Letters* 36, L16302. <http://dx.doi.org/10.1029/2009GL039297>.
- Wilson, D.S., Jamieson, S.S.R., Barrett, P.J., Leitchenkov, G., Gohl, K., Larter, R.D., 2012. Antarctic topography at the Eocene–Oligocene boundary. *Palaeogeography, Palaeoclimatology, Palaeoecology* 335–336, 24–34.
- Witts, J.D., Bowman, V.C., Wignall, P.B., Crame, J.A., Francis, J.E., Newton, R.J., 2015. Evolution and extinction of Maastrichtian (Late Cretaceous) cephalopods from the López de Bertodano Formation, Seymour Island, Antarctica. *Palaeogeography, Palaeoclimatology, Palaeoecology* 418, 193–212.
- Wood, G.D., Gabriel, A.M., Lawson, J.C., 1996. Chapter 3. Palynological techniques – processing and microscopy. In: Jansonius, J., McGregor, D.C. (Eds.), *Palynology: Principles and Applications* vol. 1. American Association of Stratigraphic Palynologists Foundation, Dallas, pp. 29–50.
- Woodburne, M.O., Case, J.A., 1996. Dispersal, vicariance and the late Cretaceous to early Tertiary land mammal biogeography from South America to Australia. *Journal of Mammalian Evolution* 3, 121–161.
- Wrenn, J.H., Beckman, S.W., 1982. Maceral, total organic carbon, and palynological analyses of Ross Ice Shelf Project Site J9 cores. *Science* 216, 187–189.
- Wrenn, J.H., Hart, G.F., 1988. Paleogene dinoflagellate cyst biostratigraphy of Seymour Island, Antarctica. In: Feldmann, R.M., Woodburne, M.O. (Eds.), *Geology and Paleontology of Seymour Island*. Geological Society of America Memoir 169, pp. 321–447.
- Zachos, J., Pagani, M., Sloan, L., Thomas, E., Billups, K., 2001. Trends, rhythms, and aberrations in global climate change 65 Ma to present. *Science* 292, 686–693.
- Zachos, J.C., Dickens, G.R., Zeebe, R.E., 2008. An early Cenozoic perspective on greenhouse warming and carbon-cycle dynamics. *Nature* 451, 279–283.
- Zinsmeister, W.J., 1998. Discovery of fish mortality horizon at the K–T boundary on Seymour Island: re-evaluation of events at the end of the Cretaceous. *Journal of Paleontology* 72, 556–571.
- Zinsmeister, W.J., Macellari, C.A., 1988. Bivalvia (Mollusca) from Seymour Island, Antarctic Peninsula. In: Feldmann, R.M., Woodburne, M.O. (Eds.), *Geology and Paleontology of Seymour Island*. Geological Society of America Memoir 169, pp. 53–284.